AGA0414
Espectroscopia multi-objeto

- Multi-object spectrographs
- *Some applications*

Prof. Jorge Meléndez

Multi-object spectroscopy

- Why ?
- How ?

R136 region in the 30 Doradus Nebula. © Nasa

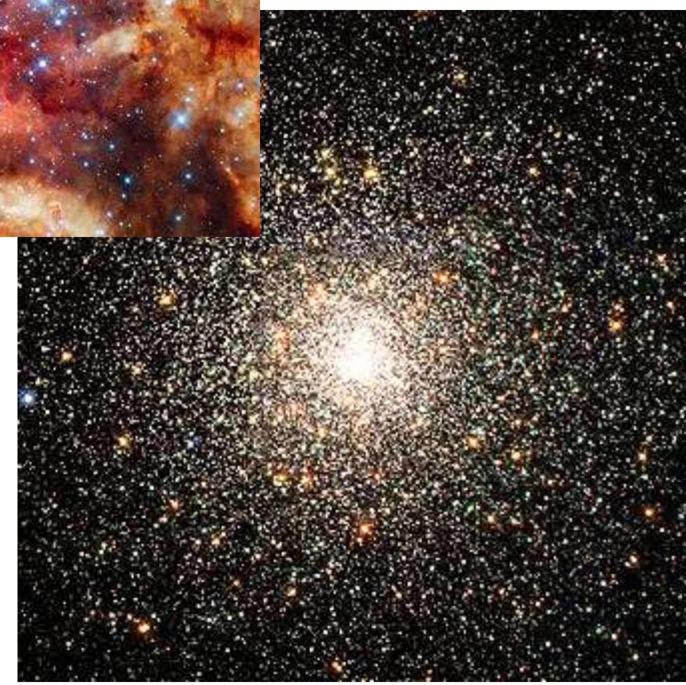

M80, HST

Multi-object spectroscopy

Put more than 1 object on the slit !

PROPERTIES OF THE GALACTIC NUCLEUS IN THE DIRECTION OF NGC 6522

HALTON ARP
Mount Wilson and Palomar Observatories Carnegie Institution of Washington
California Institute of Technology

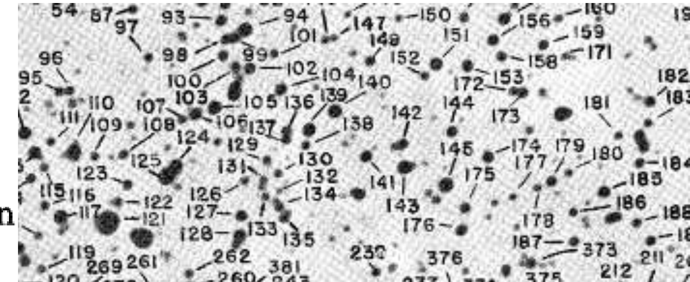

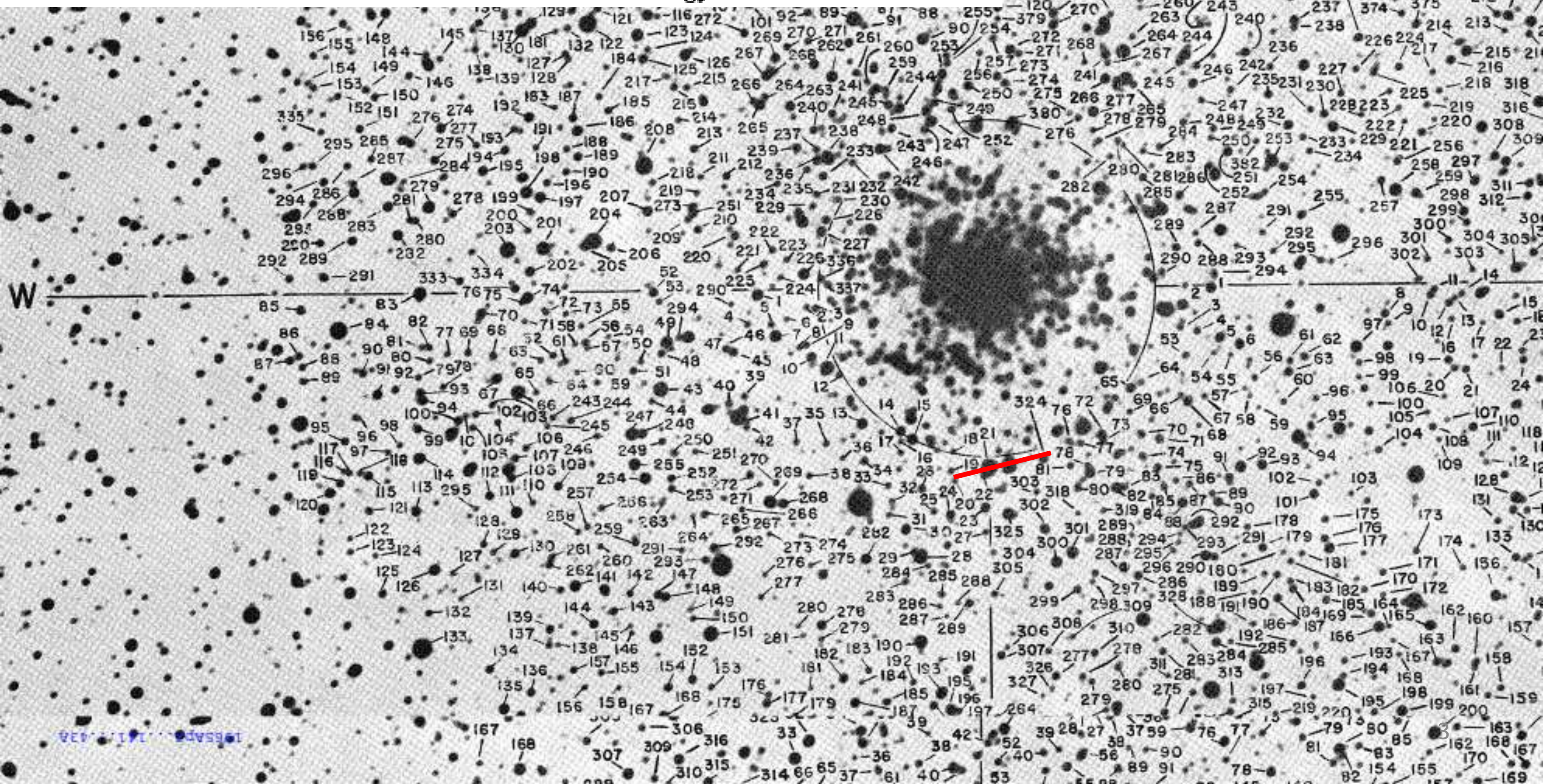

Position angle : do N para o E, S, O

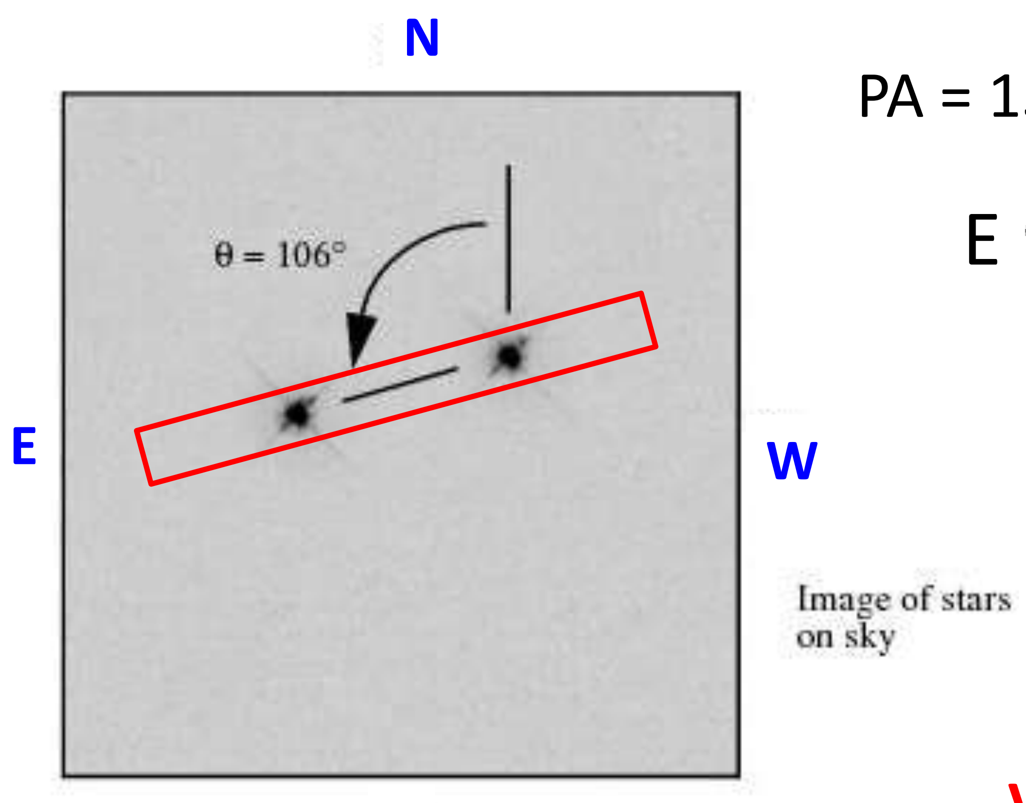

Binary system

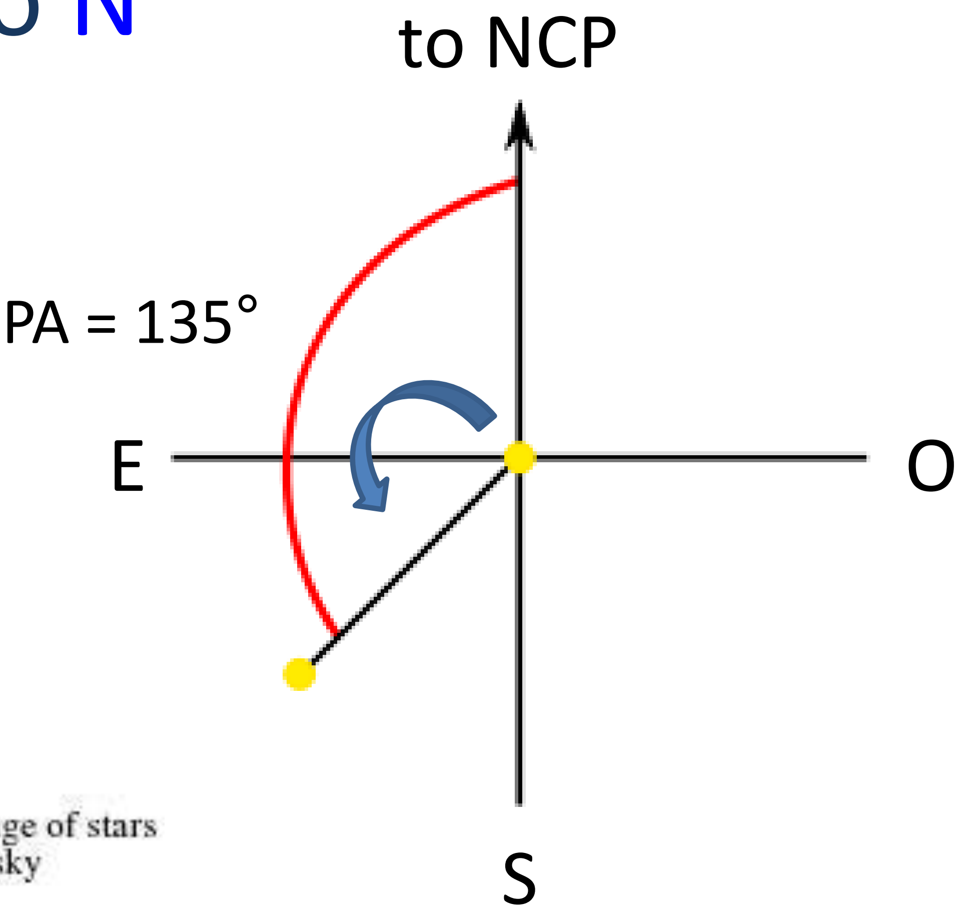

Verificar sempre se a mesma definição (N → E.S.O.) é usada pelo instrumento

Position angle

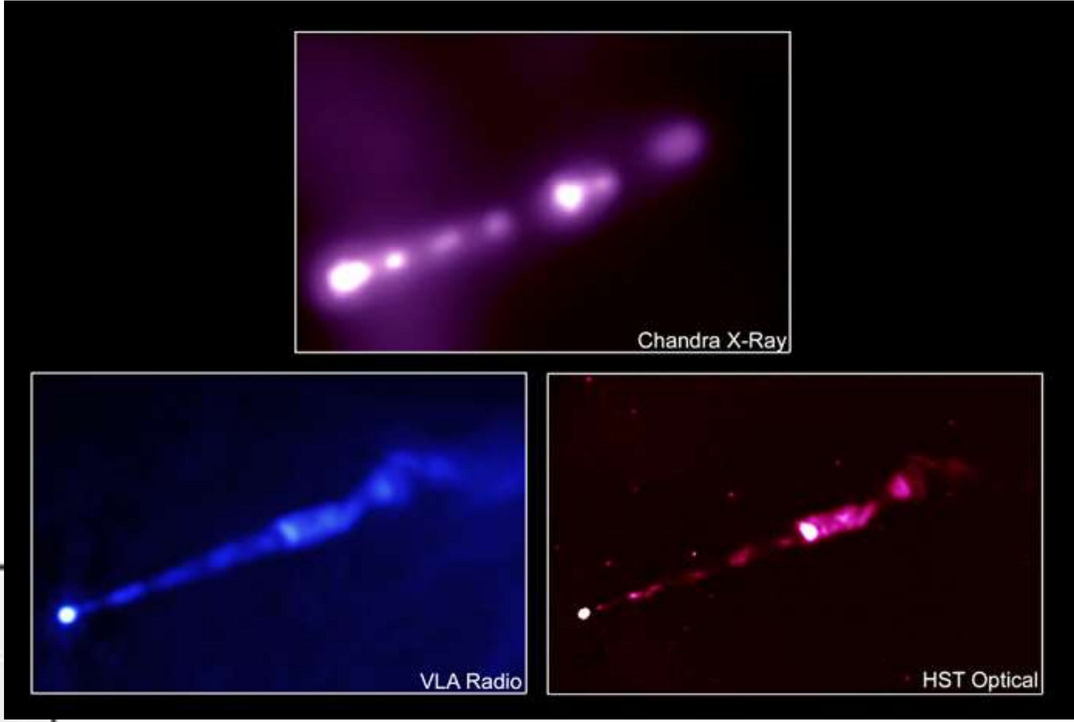

N

E

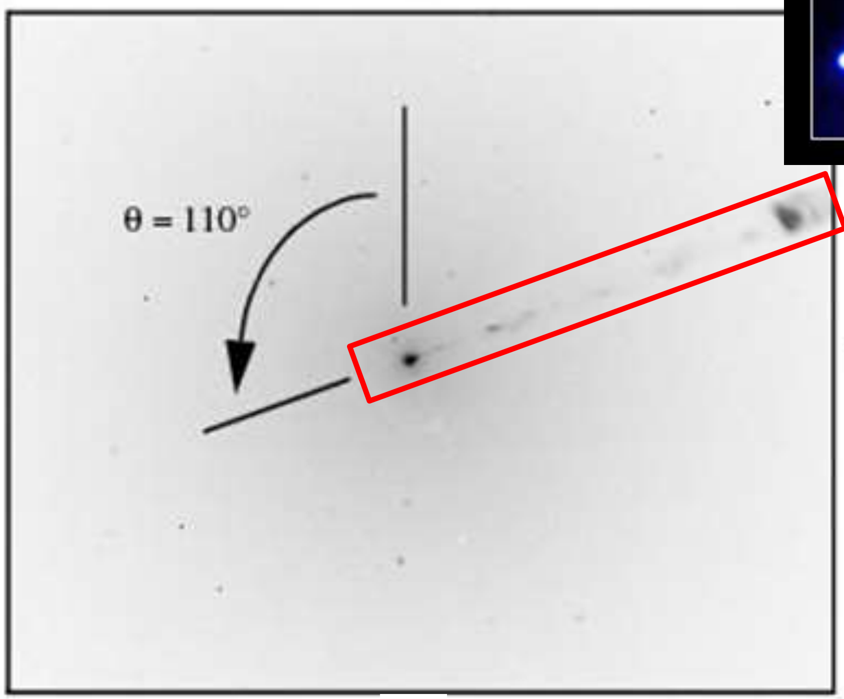

W

S

Radio galaxy with jet

Radio Galaxy (Virgo A) with jet

Observing bulge stars in the infrared with Phoenix : *Echelle* mas apenas uma ordem …

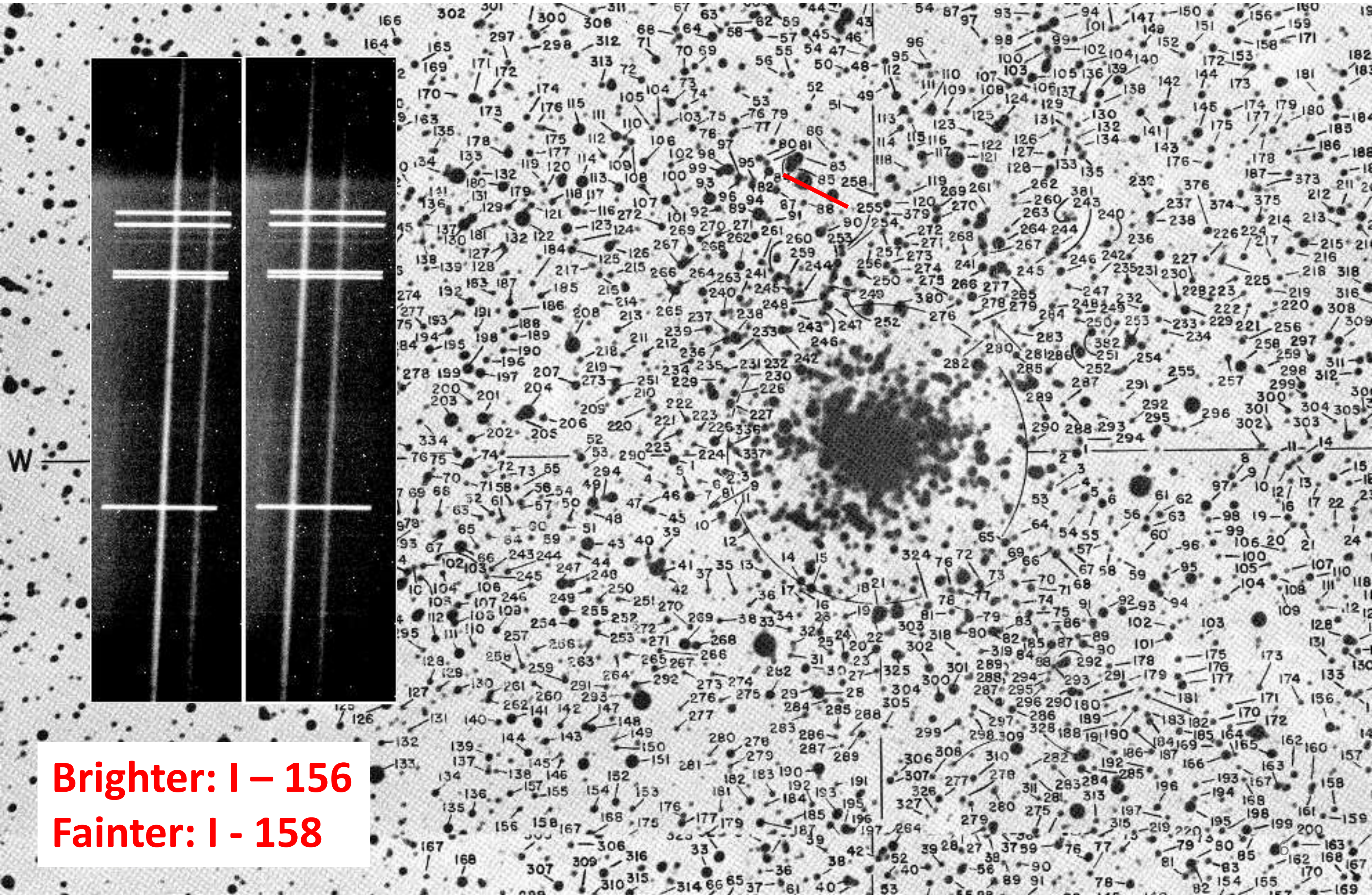

A&A 484, L21–L25 (2008)
DOI: 10.1051/0004-6361:200809398

117 citations

Astronomy & Astrophysics

Letter to the Editor

Chemical similarities between Galactic bulge and local thick disk red giant stars

J. Meléndez[1,2], M. Asplund[3], A. Alves-Brito[4], K. Cunha[5,6], B. Barbuy[4], M. S. Bessell[2], C. Chiappini[7,8], K. C. Freeman[2], I. Ramírez[9], V. V. Smith[5], and D. Yong[2]

High resolution IR spectroscopy with Phoenix at Gemini

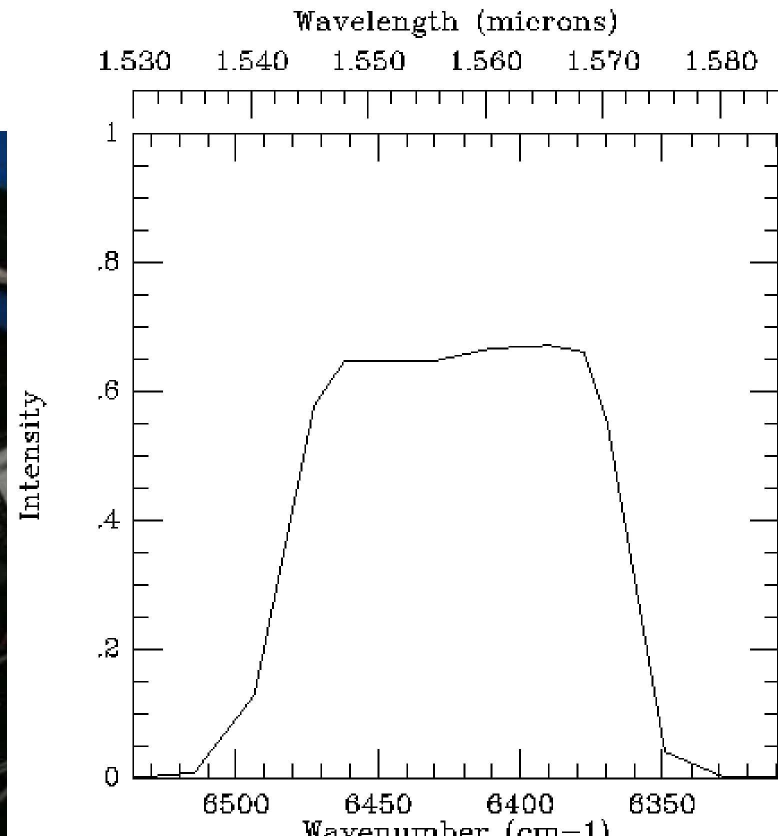

Data reduction in the infrared : one star

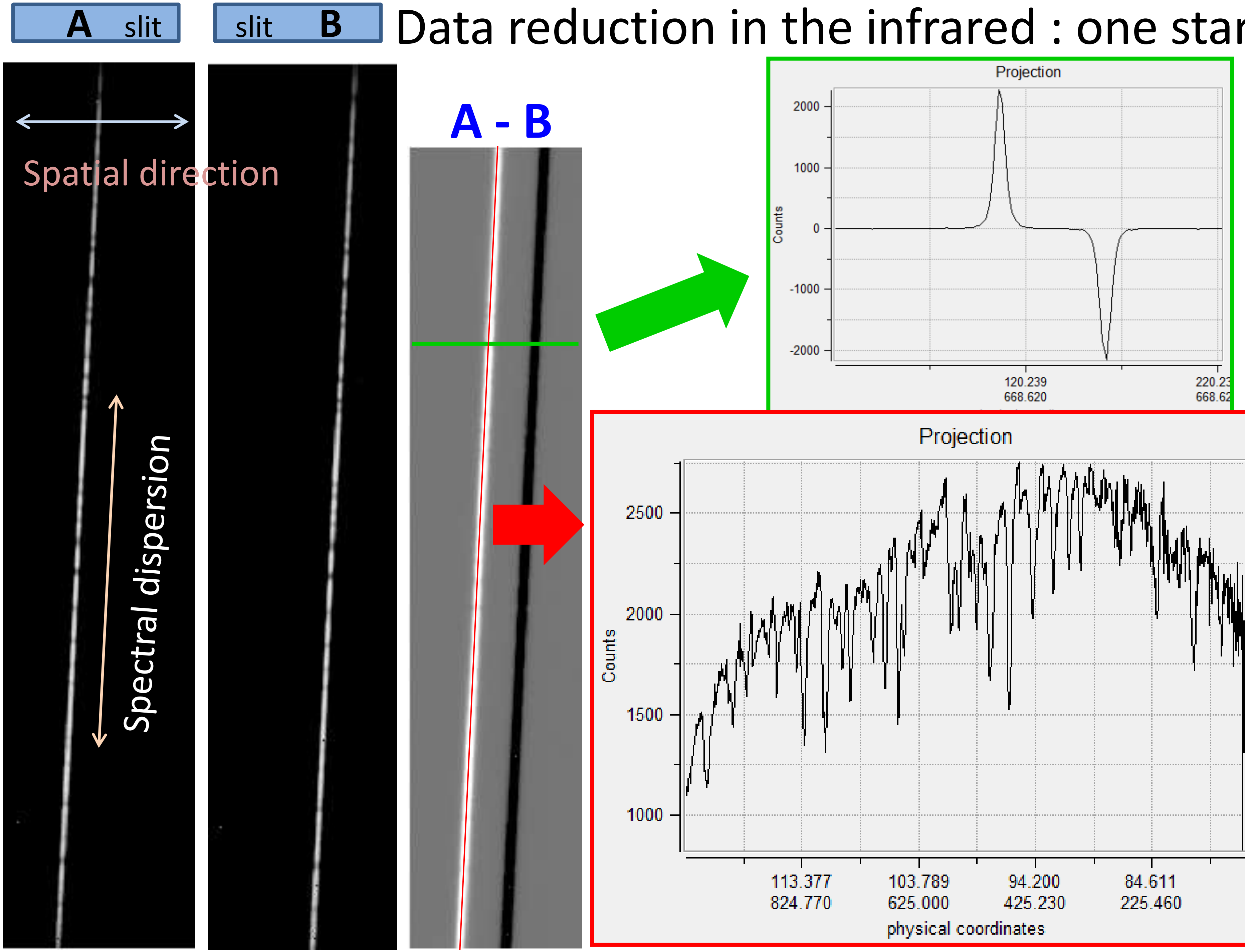

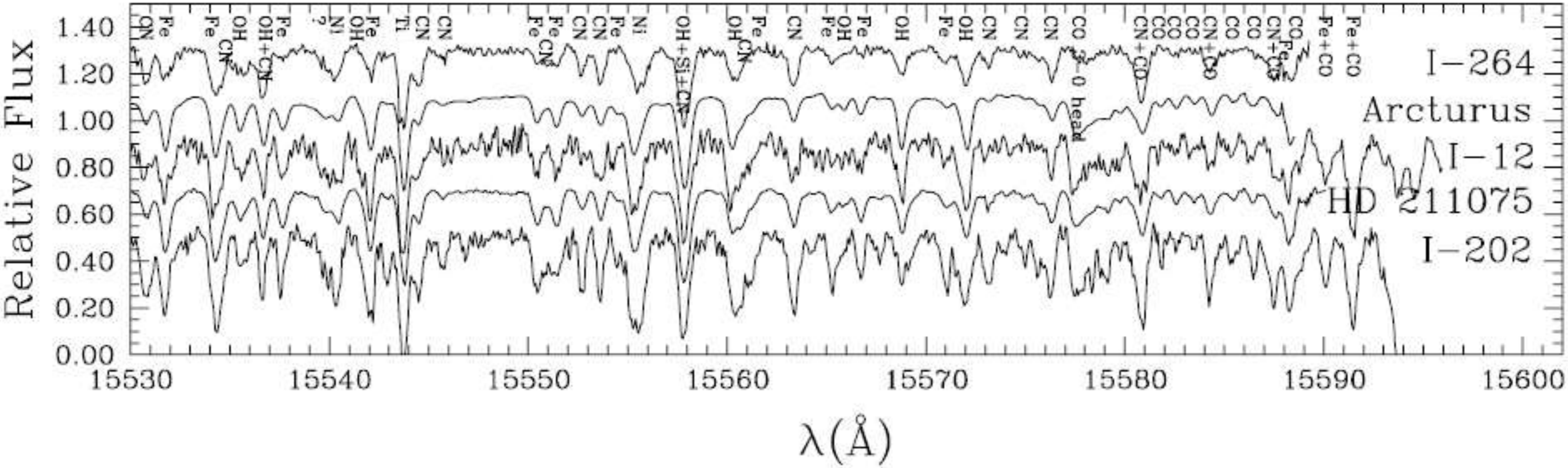

Fig. 1. Observed Phoenix spectra of selected bulge giants as well as thick (Arcturus = HD 124897) and thin (HD 211075) disk stars.

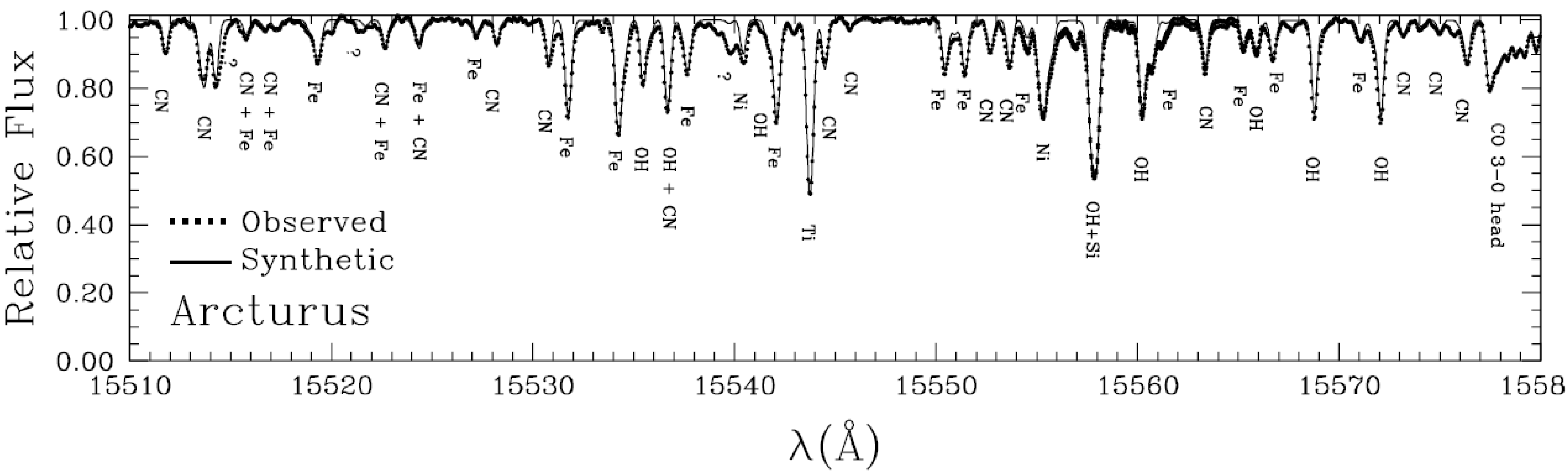

Fig. 7. Observed (dotted line) and synthetic (solid line) spectra of Arcturus in the region 1.551–1.558 μm.

Long slit (*fenda longa*) spectroscopy

Corte na direção espacial para PA = 43°

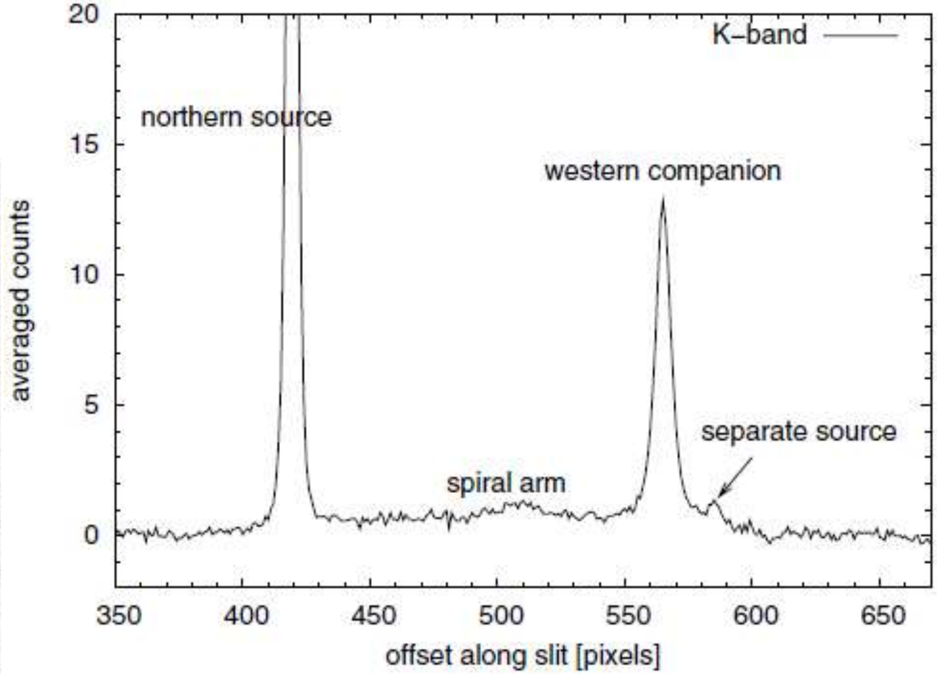

Fig. 4. Cut along the spatial axis of the two-dimensional *K*-band spectrum obtained for the PA = +43° setting (see Fig. 2). The cut consists of an average over almost all the spatial lines of the image.

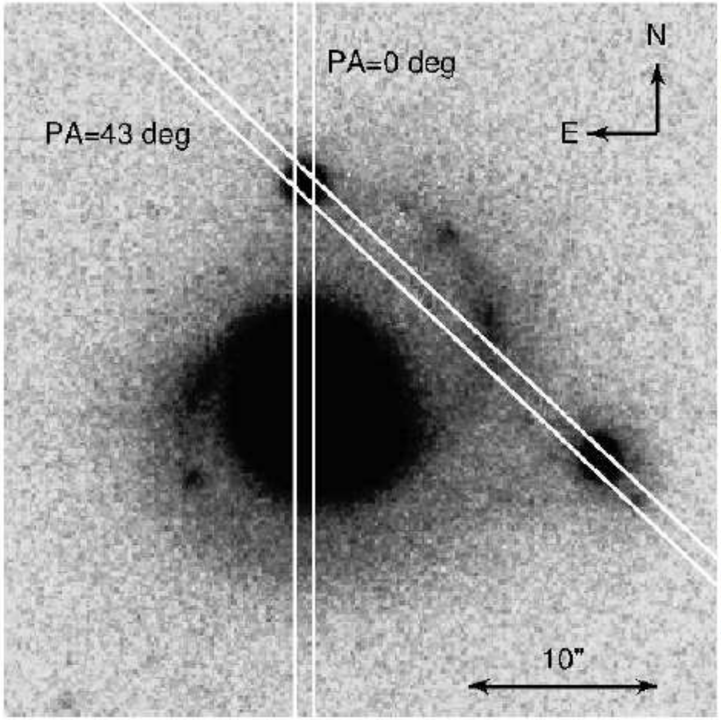

Fig. 2. ISAAC *J*-band image of I Zw 1 overlaid with the two slit settings used for the ISAAC long-slit spectroscopy. The slit for PA = 0° includes the QSO of I Zw 1 and the northern source, the slit for PA = 43° includes the northern source and the likely western companion.

Fenda no plano focal

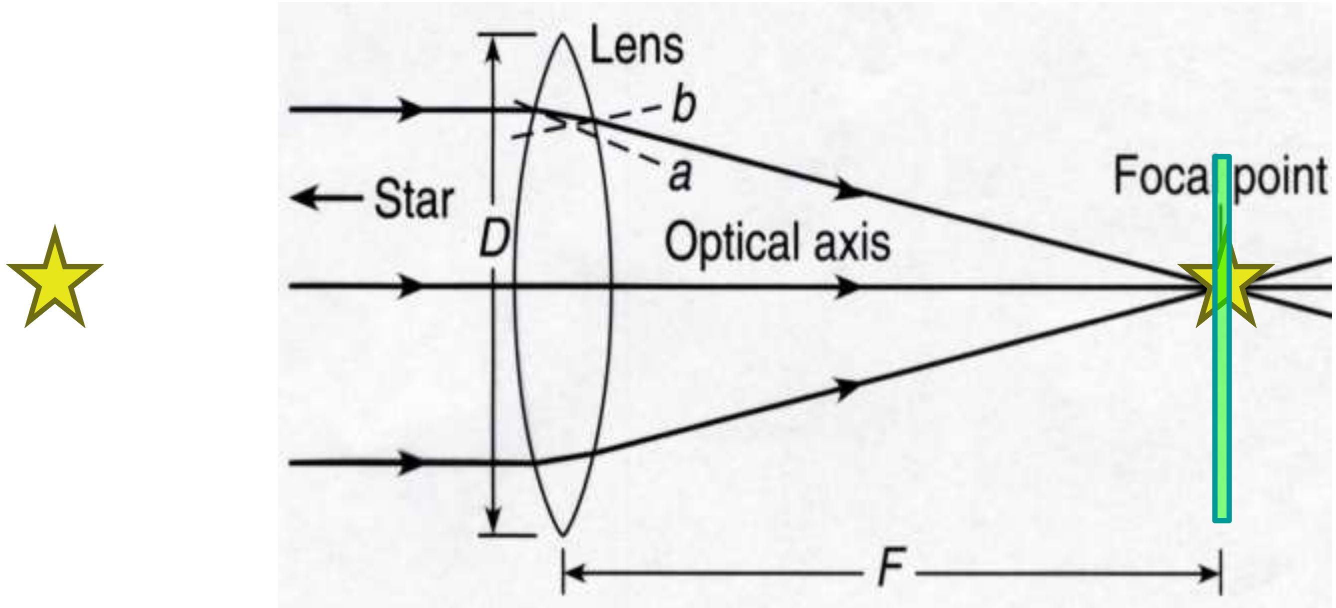

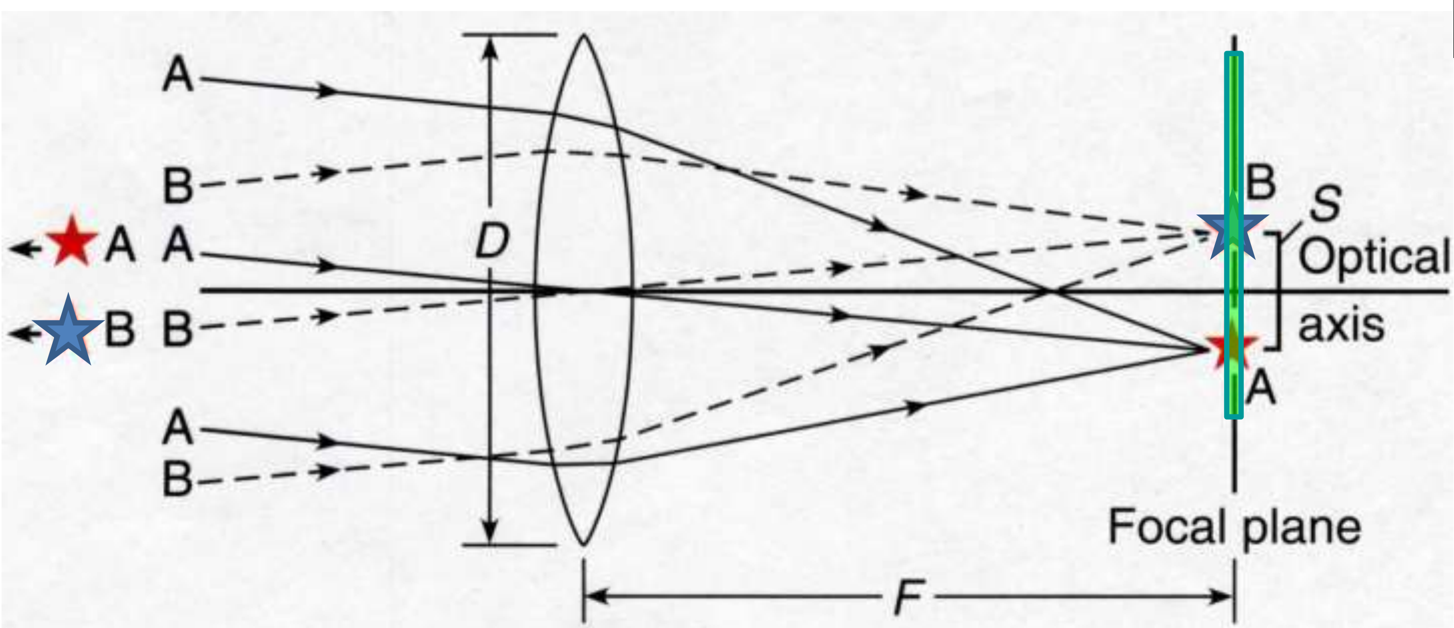

Spectral dispersion

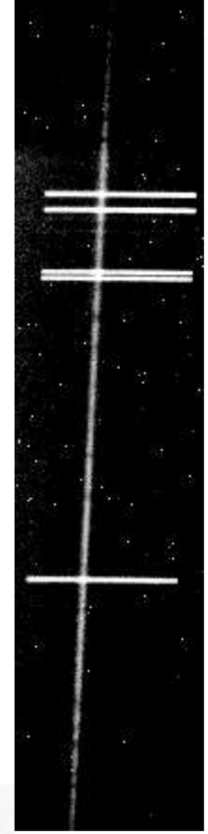

Sky lines

Spatial direction

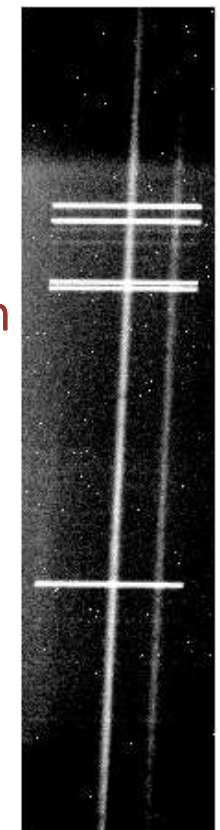

Multi-slit spectroscopy

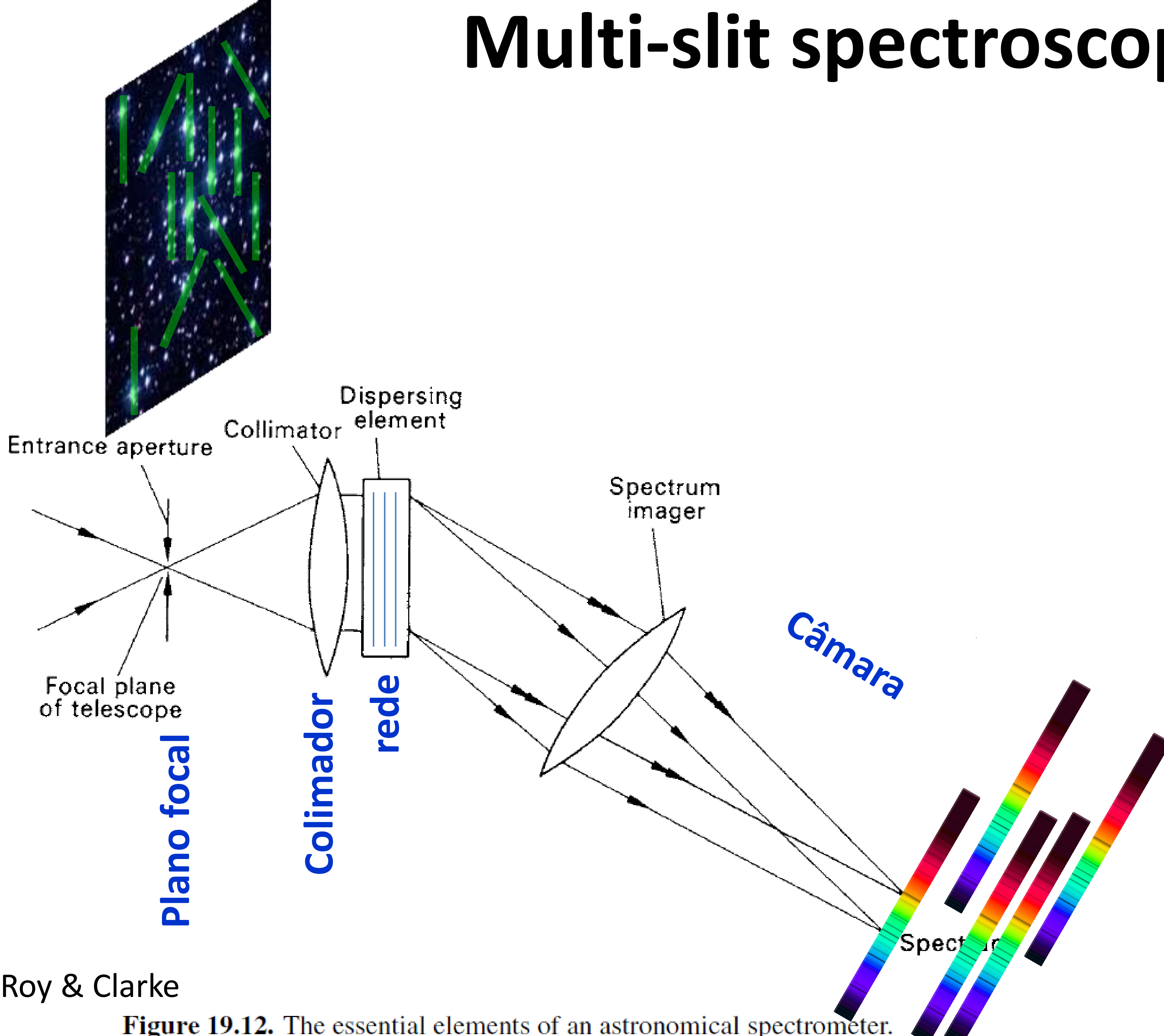

Figure 19.12. The essential elements of an astronomical spectrometer.

Multi-slit spectroscopy

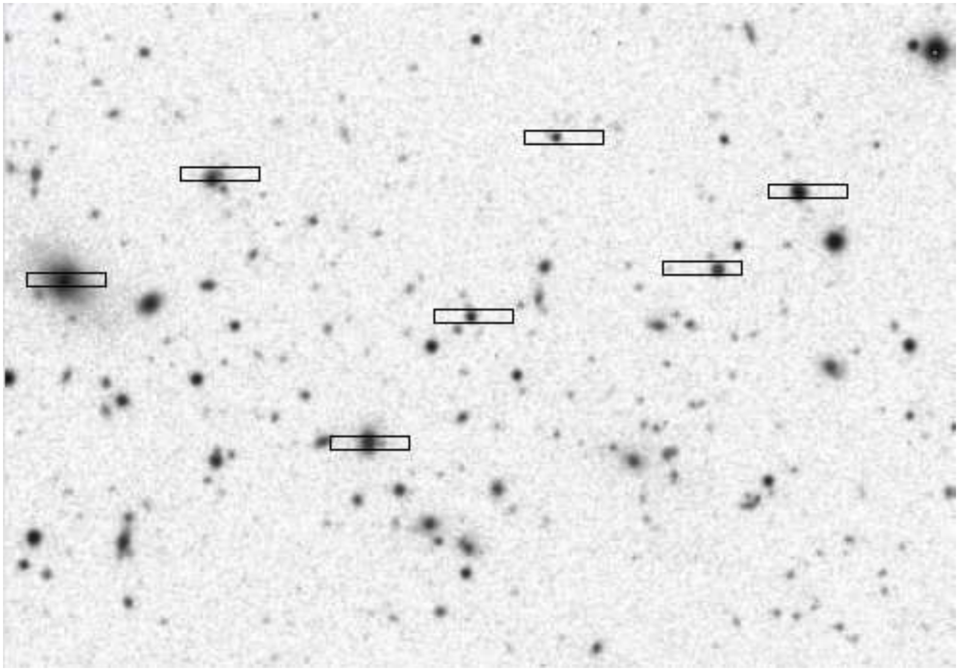

Slits at the focal plane

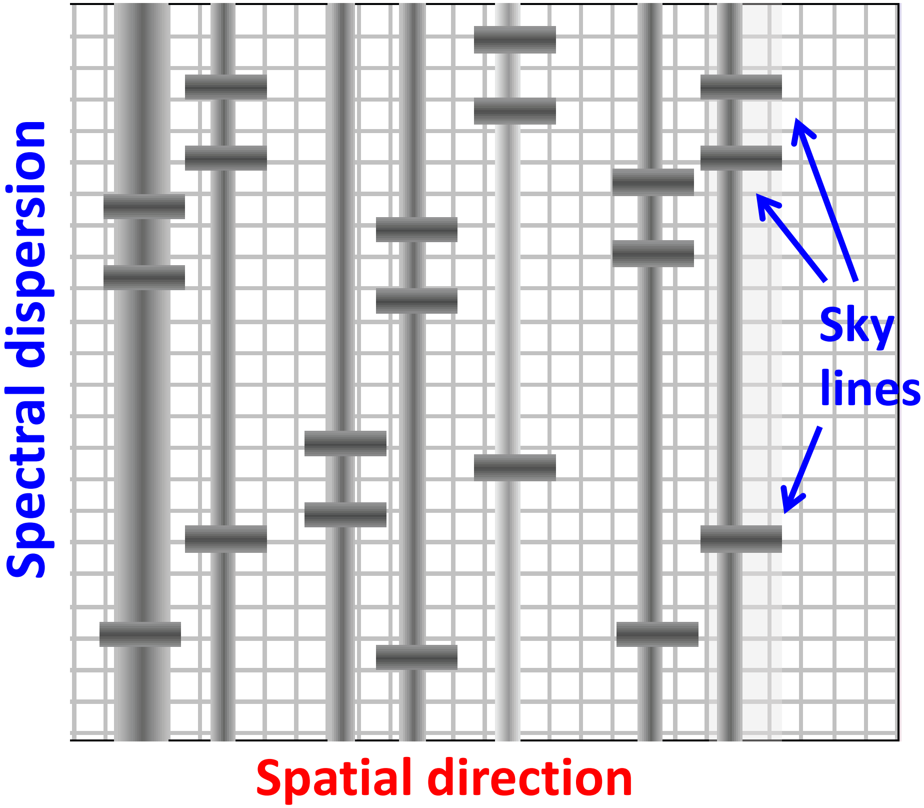

Spectra on the CCD

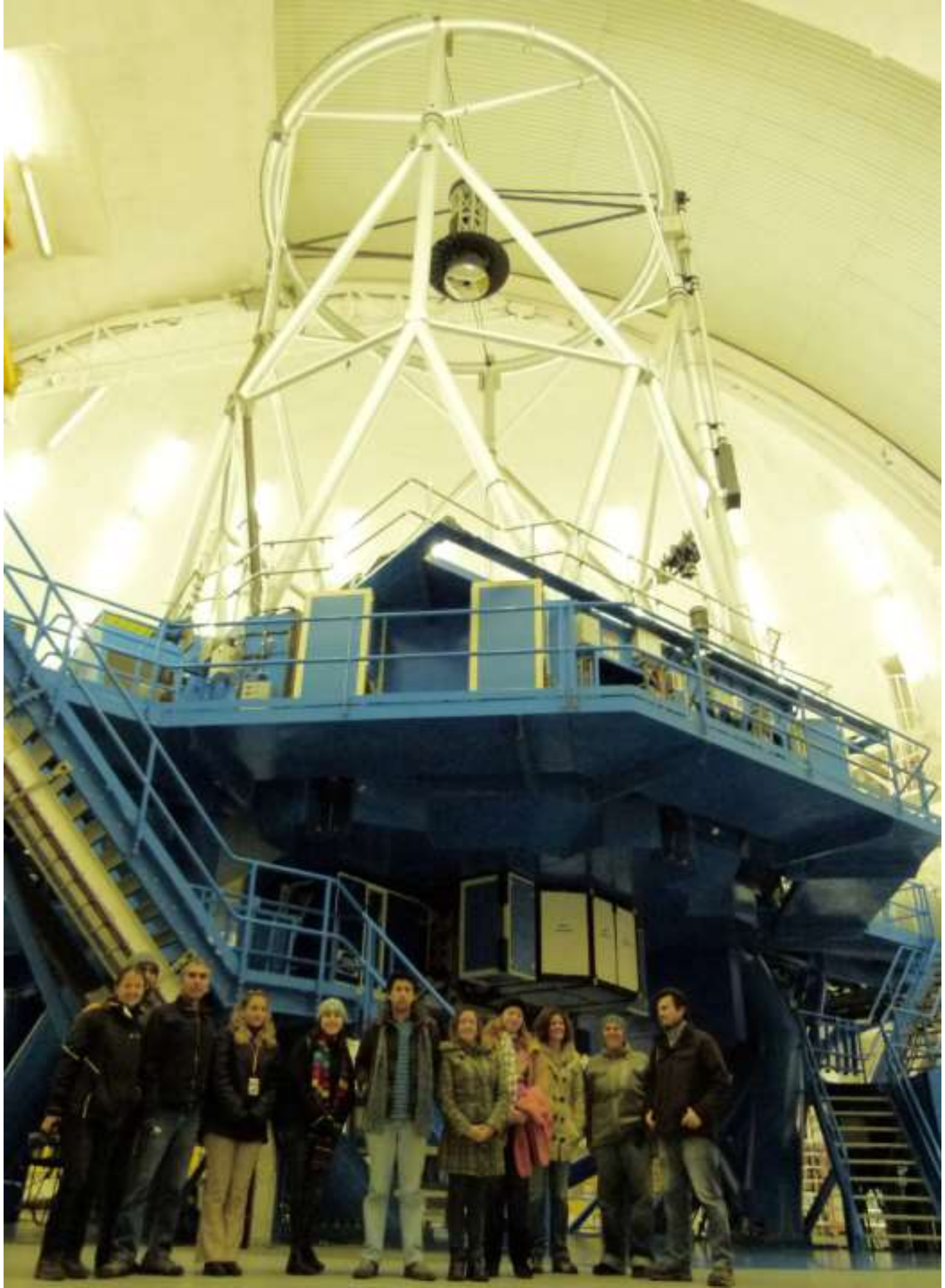

GMOS

Gemini
Multi-**O**bject
Spectrograph

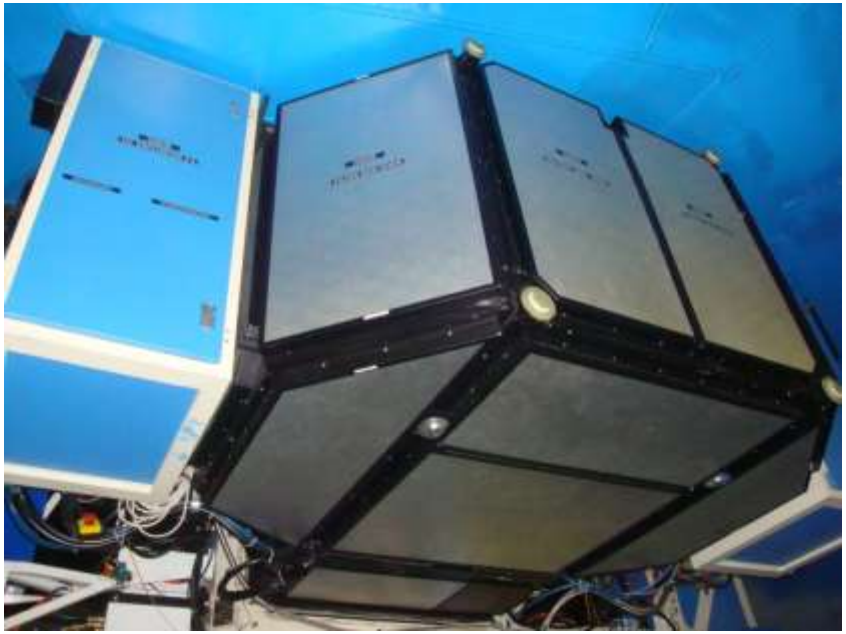

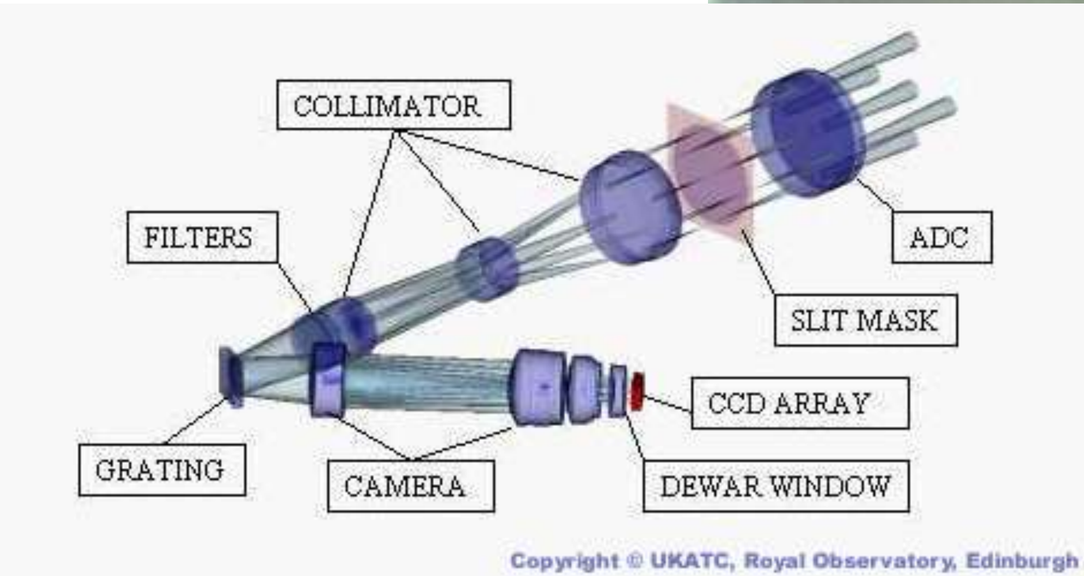
COLLIMATOR
FILTERS
ADC
SLIT MASK
CCD ARRAY
GRATING
CAMERA
DEWAR WINDOW
Copyright © UKATC, Royal Observatory, Edinburgh

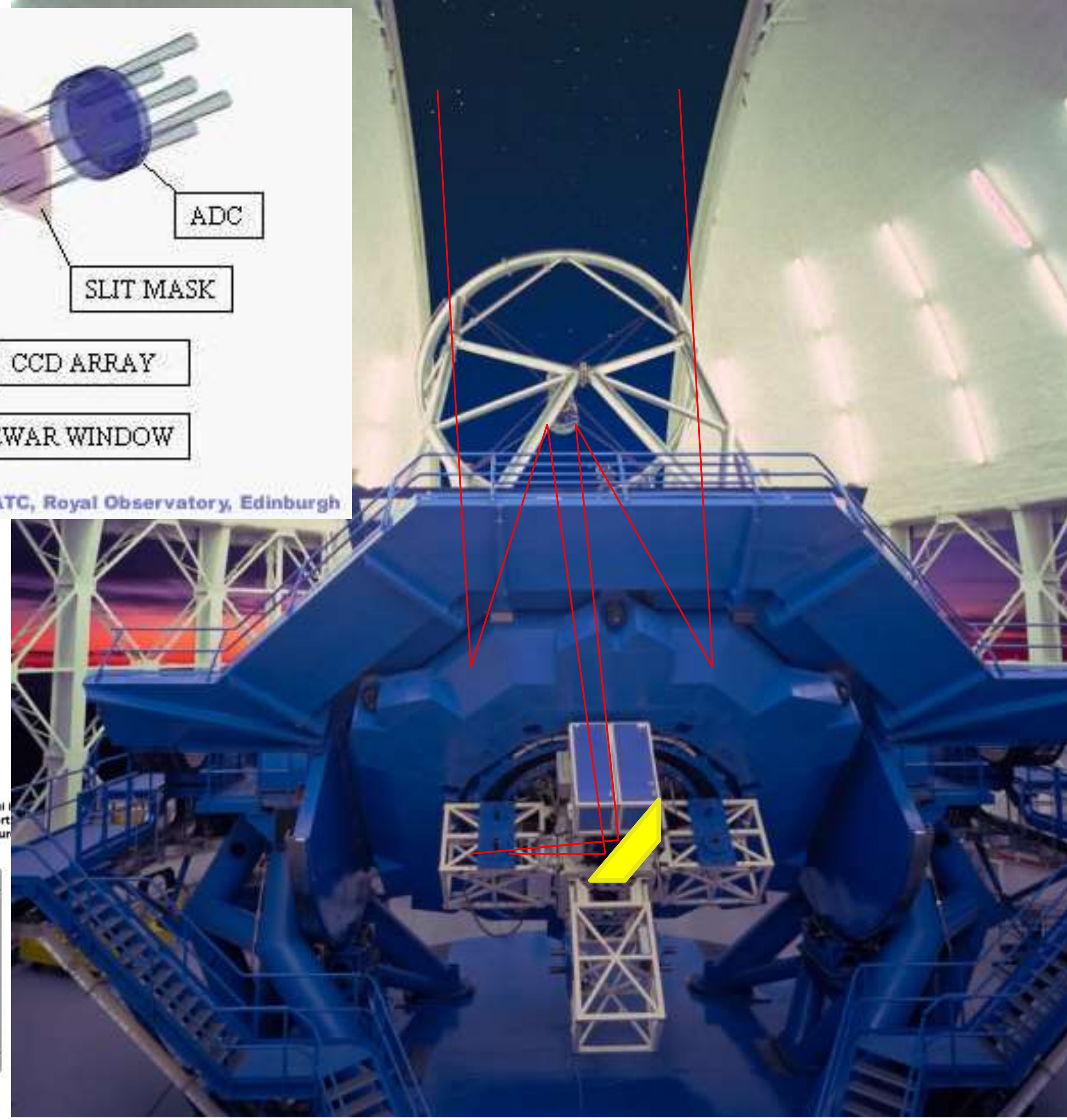

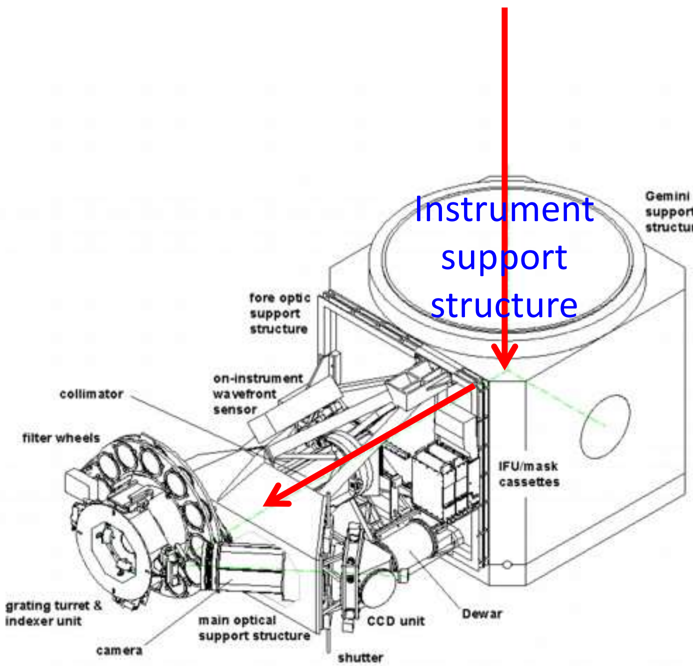
Instrument support structure
fore optic support structure
on-instrument wavefront sensor
collimator
filter wheels
IFU/mask cassettes
grating turret & indexer unit
main optical support structure
CCD unit
Dewar
camera
shutter

GMOS

- 2 **G**emini **M**ulti-**O**bject **S**pectrographs : GN & GS
- 5.5 arcminute field of view
- Imaging
- 0.36-0.94 μm long-slit spectroscopy
- 0.36-0.94 μm multi-slit spectroscopy
- Integral Field Unit (IFU), to obtain spectra from a 35 $arcsec^2$ area with a sampling of 0.2 arcsec

Camera Properties

Home » Sciops » Instruments » GMOS » Imaging

- *Commissioning of the e2v DD devices expected late in semester 2011B
- *Pixel Scale to be confirmed when the CCDs are commissioned, expected for late 2012 / early 20

Instrument	Pixel Size (arcsec)	Imaging Field of View ($arcsec^2$)	Throughput
GMOS-N (original EEV and upgraded e2v DD*)	0.0728	330 x 330	data / plot
GMOS-N (Hamamatsu*)	0.0809		
GMOS-S (original EEV)	0.0730	330 x 330	

GMOS imaging field = 5,5 x 5,5 arcmin

GMOS imaging

NGC 628 = M 74

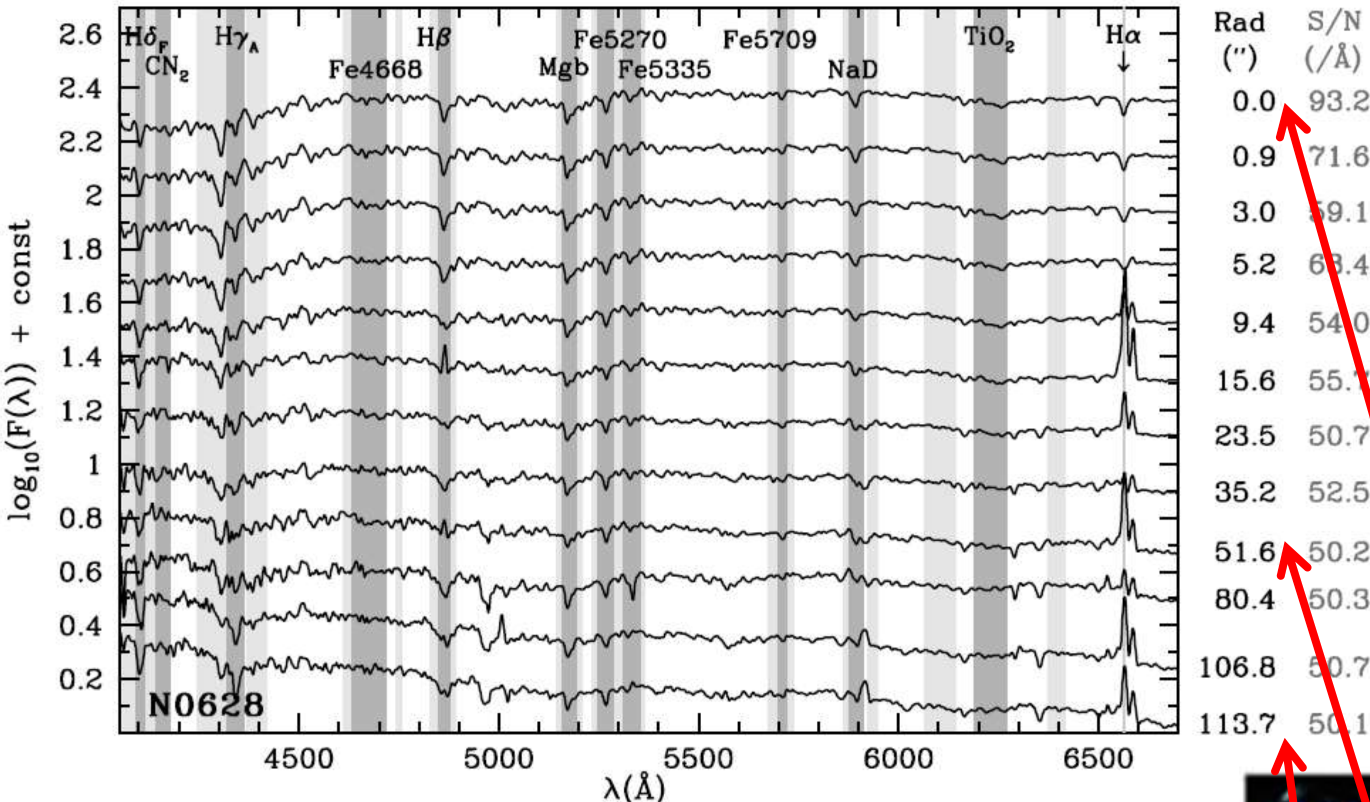

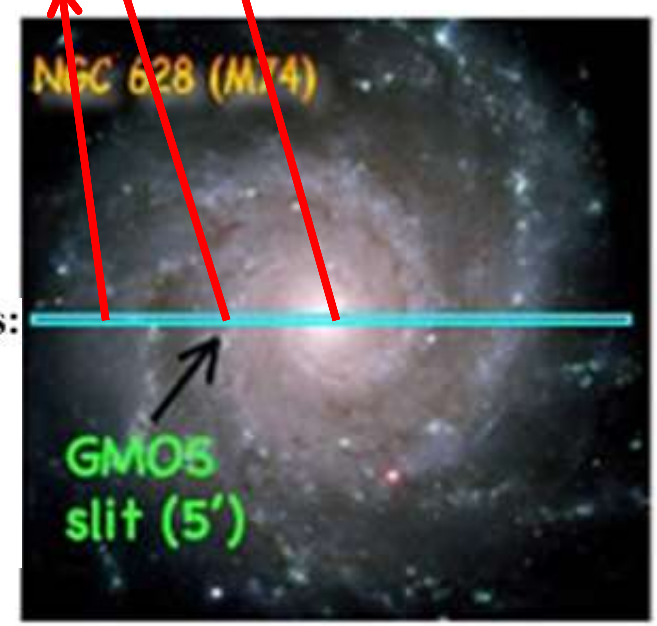

GMOS long-slit

2009 MNRAS, 395, 28

Stellar Population and Kinematic Profiles In Spiral Bulges & Disks: Population Synthesis of Integrated Spectra

Lauren A. MacArthur[1]*, J. Jesús González[2]†, and Stéphane Courteau[3]‡

[1] Department of Astrophysics, California Institute of Technology, MS 105-24, Pasadena, CA 91125

[2] Instituto de Astronomia, Universidad Nacional Autónoma de México, Apdo Postal 70-264, Cd. Universitaria, 04510 México

[3] Department of Physics, Engineering Physics & Astronomy, Queen's University, Kingston, ON K7L 3N6, Canada

The Astrophysical Journal Supplement Series, 56:257–281, 1984 October

A LIBRARY OF STELLAR SPECTRA

George H. Jacoby and Deidre A. Hunter
Carol A. Christian

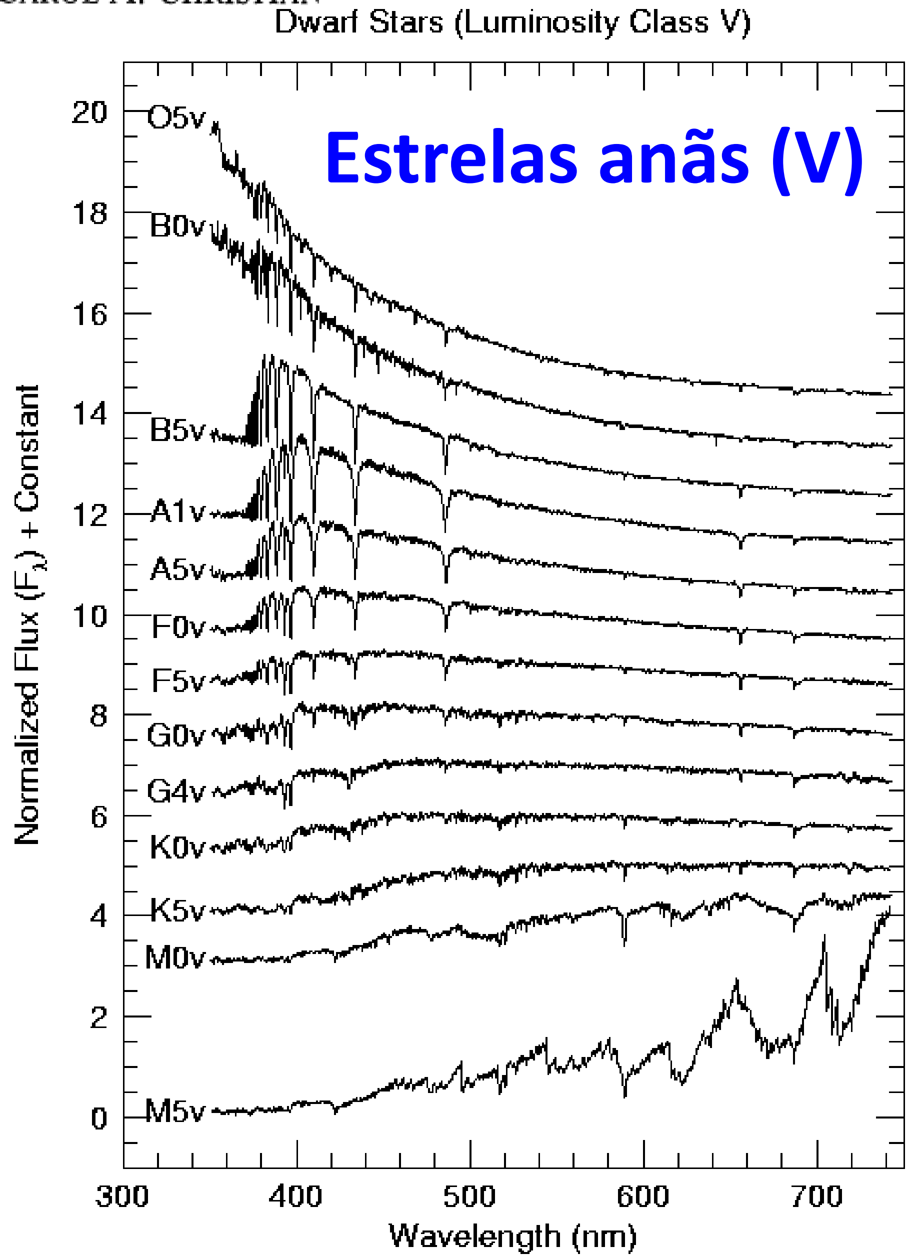

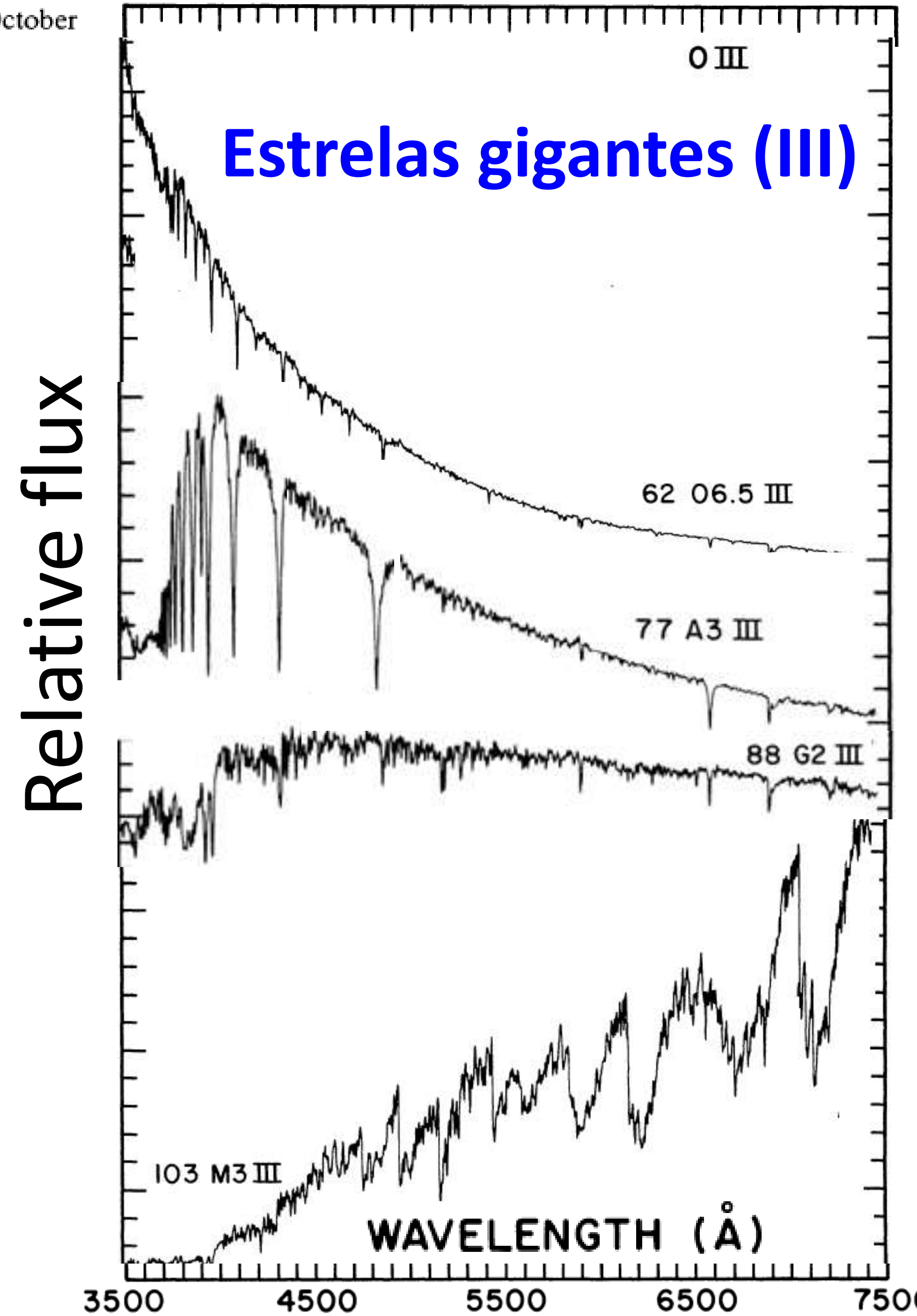

Salaris & Cassisi 2005

Absolute flux

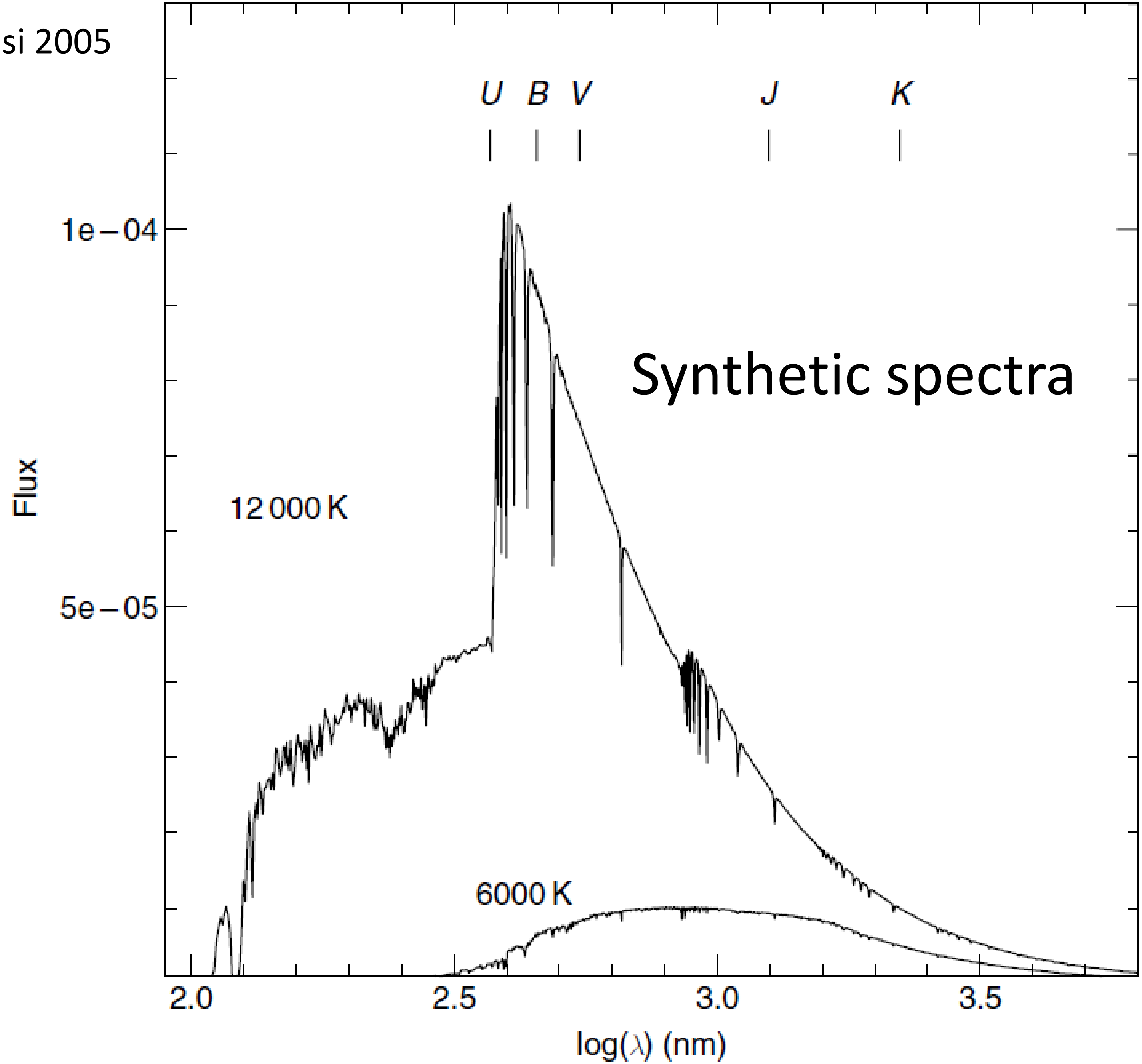

Figure 8.2 Comparison of the energy fluxes (units of erg cm^{-2} s^{-1} hz^{-1} ster^{-1}) emitted by two stars with the same solar chemical composition and solar gravity, and two different values of T_{eff}. The effective wavelength of some photometric filters is also marked

3 From theoretical models of stars, you could construct a film to show how the H–R diagram of a star cluster changes as it ages. You can then compare theory (left) with observation (right) to understand how stars evolve. Note that the time step for each frame in this film increases by a factor of 10.

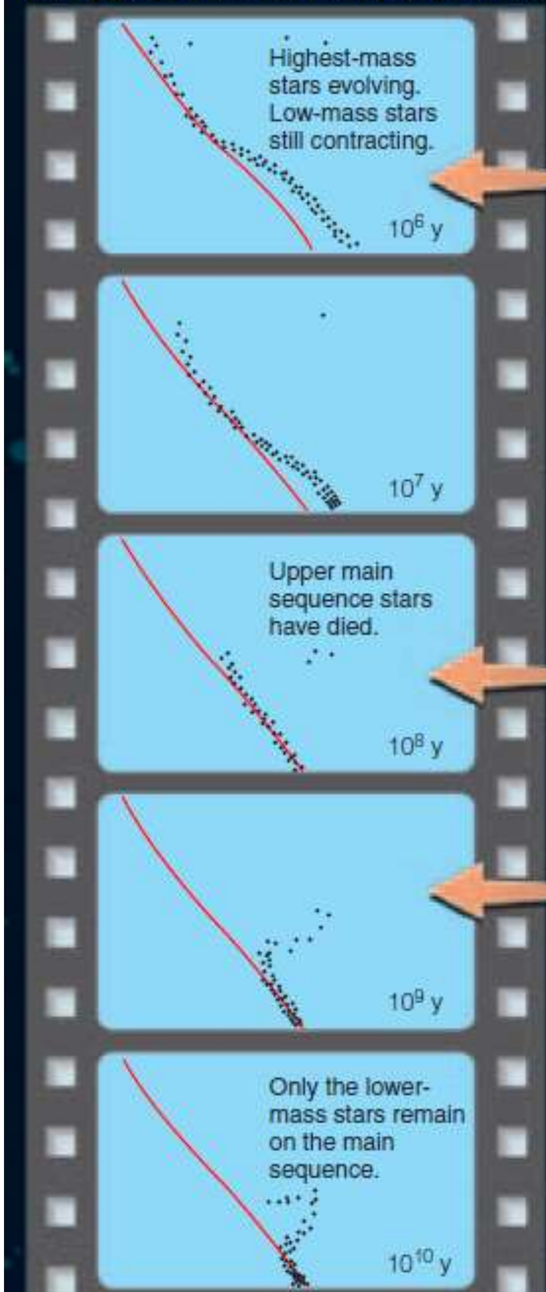

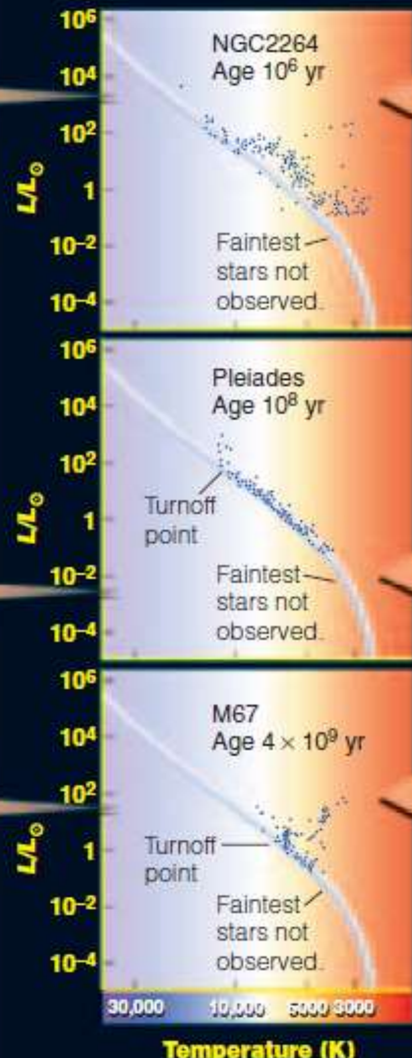

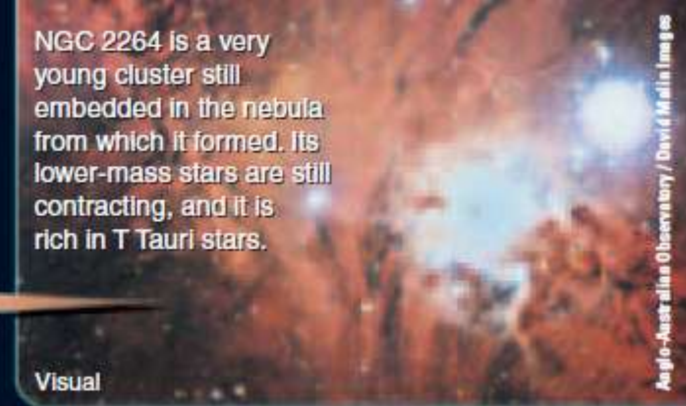

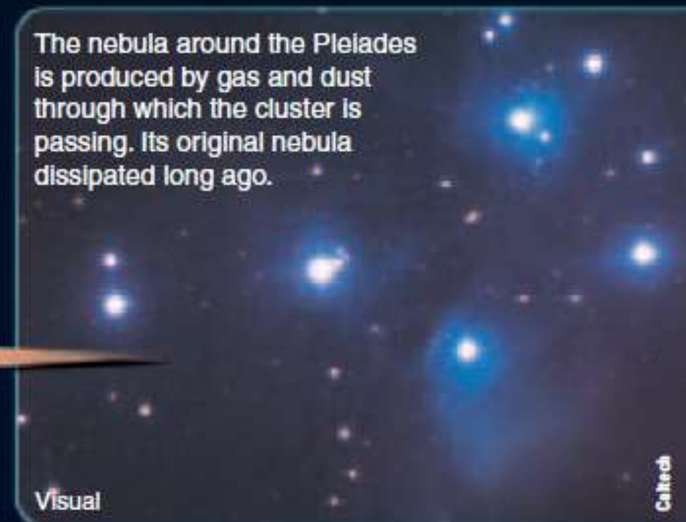

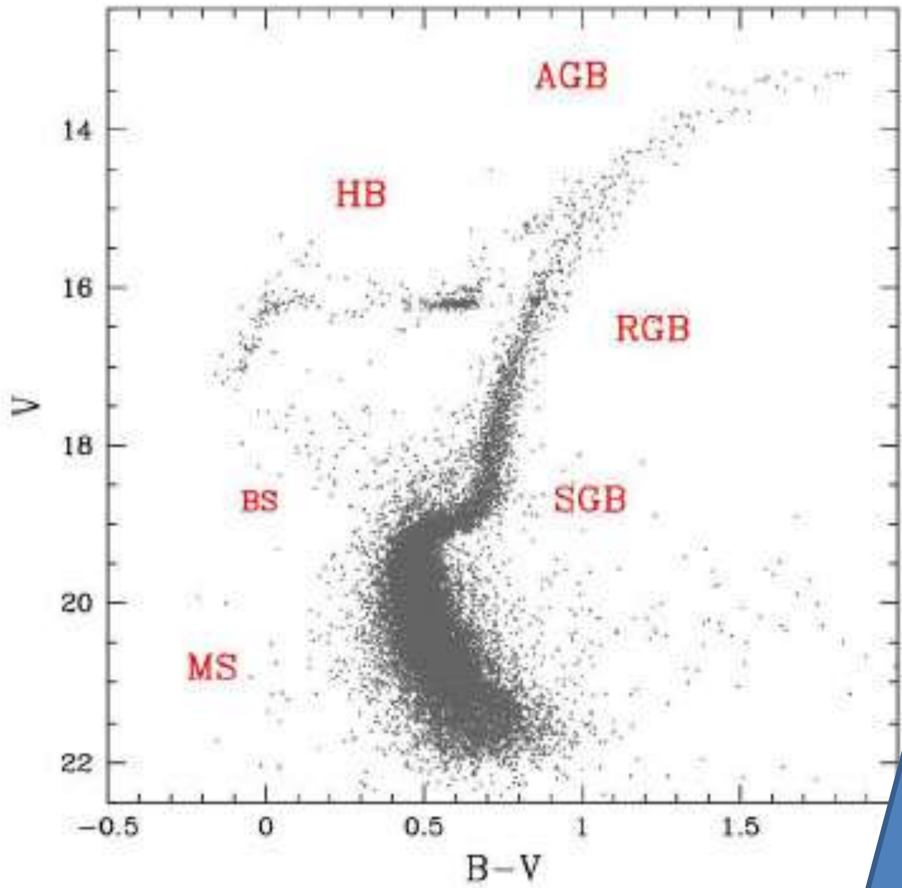

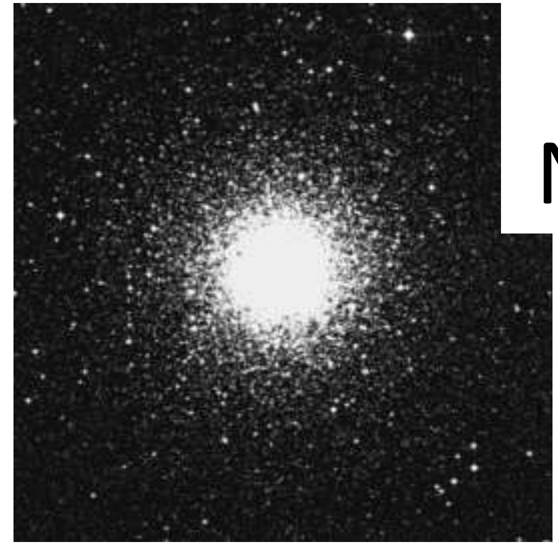

Cluster
NGC 1851

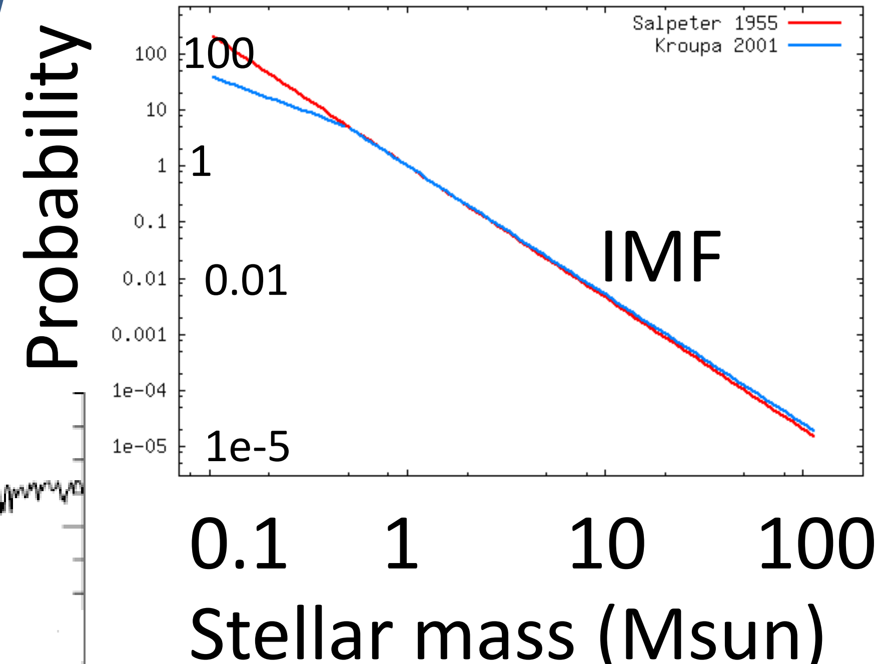

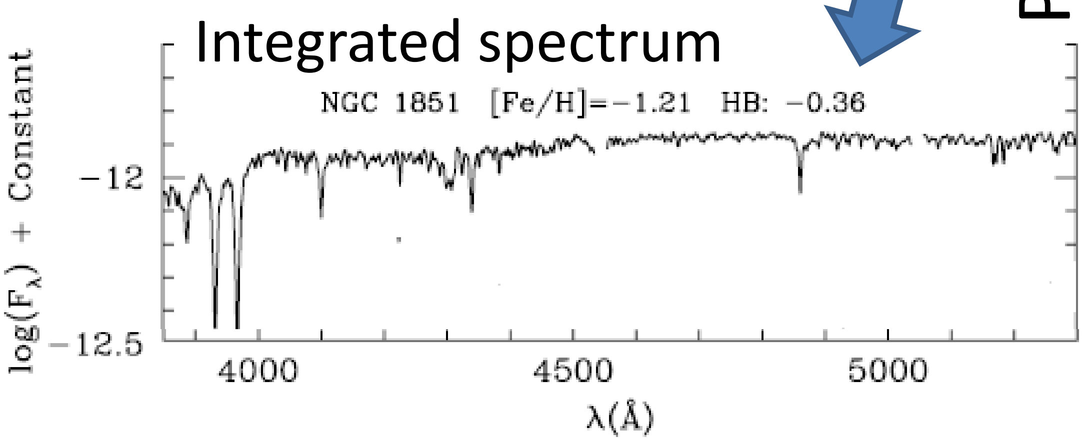

simple stellar populations (SSP) models
para várias metalicidades e idades

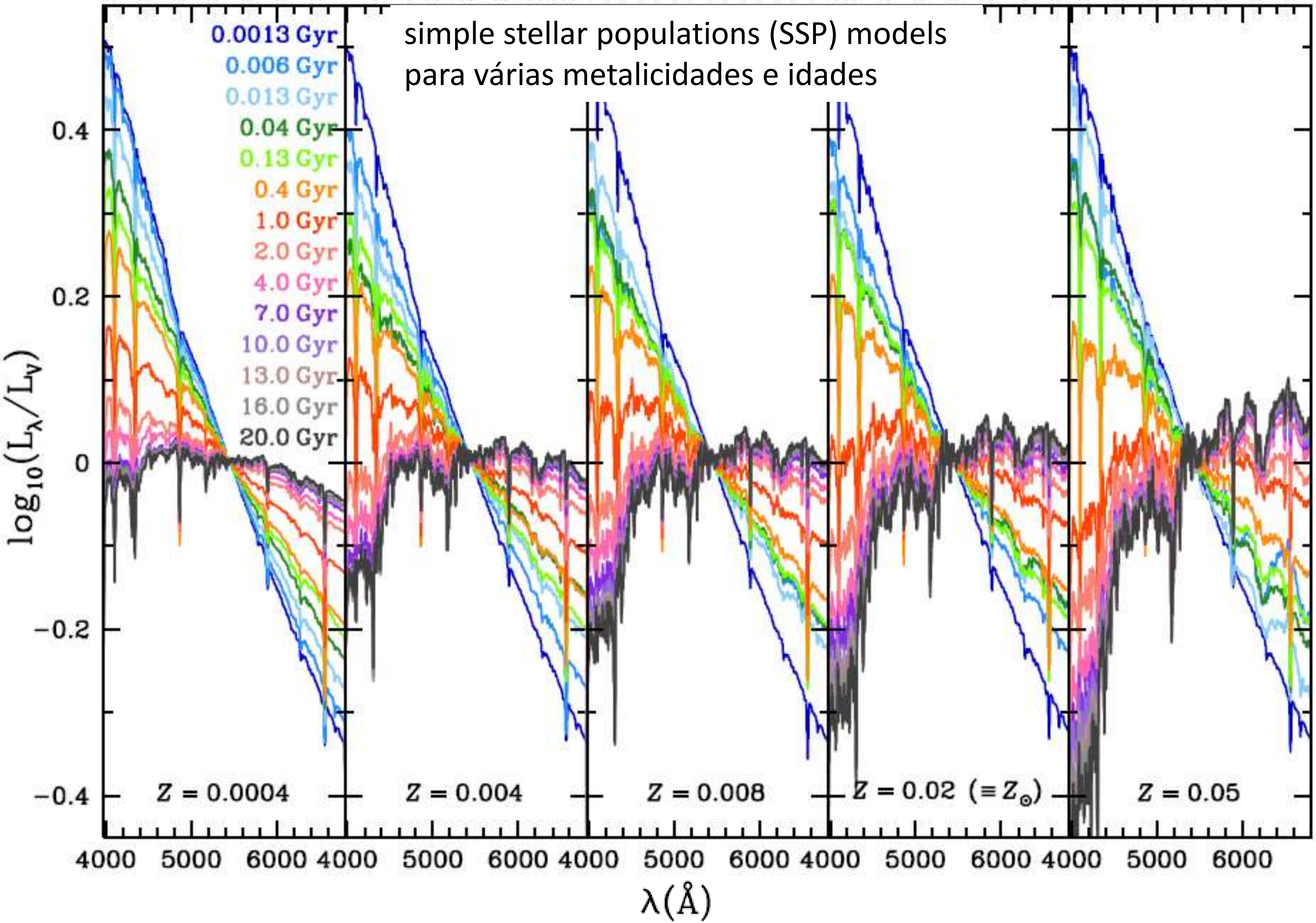

Figure 2. Spectra of the 70 SSP templates used in the population synthesis fits. Metallicity increases from left to right. Different ages have different colours and are labeled in leftmost panel. All spectra are normalized to their V-band flux.

MacArthur et al. 2009

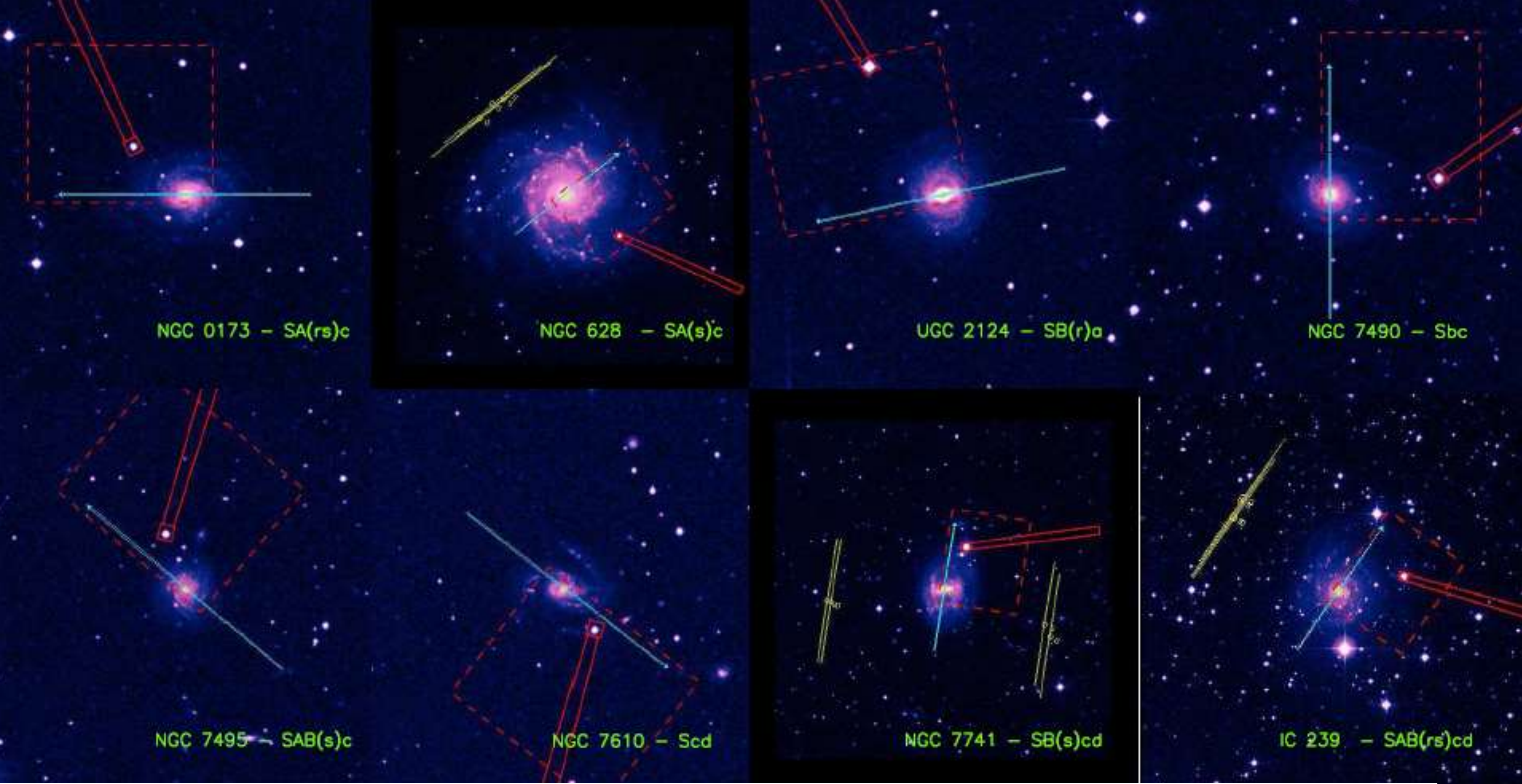

Figure 1. Observational set-up for the eight galaxies in our sample. The background images are from the Canadian Astronomy Data Centre's Digitized Sky Server (CADC; http://cadcwww.dao.nrc.ca/). The blue line represents the slit, the red (dashed) box and long arm represent the FOV of the GMOS wavefront sensor camera, with the box at the end of the arm centered on the guide star. The panels for large galaxies (NGC 628, NGC 7741, and IC 239) also show, as yellow lines, the sky offset positions. The FOV for the CADC pictures differ in all the panels but the slit length is everywhere the same (5′).

2009 MNRAS, 395, 28

Stellar Population and Kinematic Profiles In Spiral Bulges & Disks: Population Synthesis of Integrated Spectra

Lauren A. MacArthur[1*], J. Jesús González[2†], and Stéphane Courteau[3‡]
[1]Department of Astrophysics, California Institute of Technology, MS 105-24, Pasadena, CA 91125
[2]Instituto de Astronomia, Universidad Nacional Autónoma de México, Apdo Postal 70-264, Cd. Universitaria, 04510 México
[3]Department of Physics, Engineering Physics & Astronomy, Queen's University, Kingston, ON K7L 3N6, Canada

GMOS long-slit

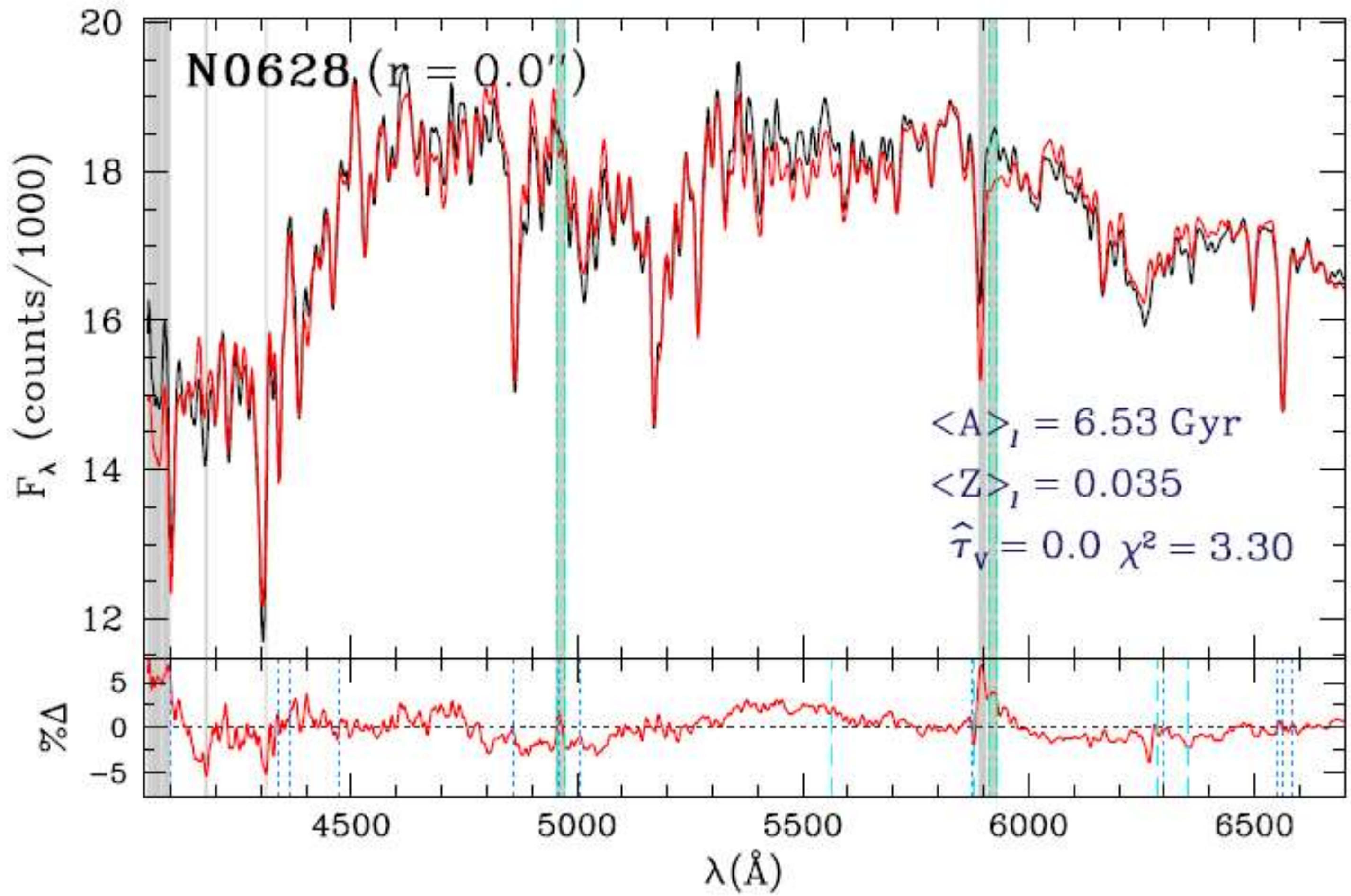

Figure 3. Central observed spectra (black) and full population synthesis fit (red)

GMOS long-slit

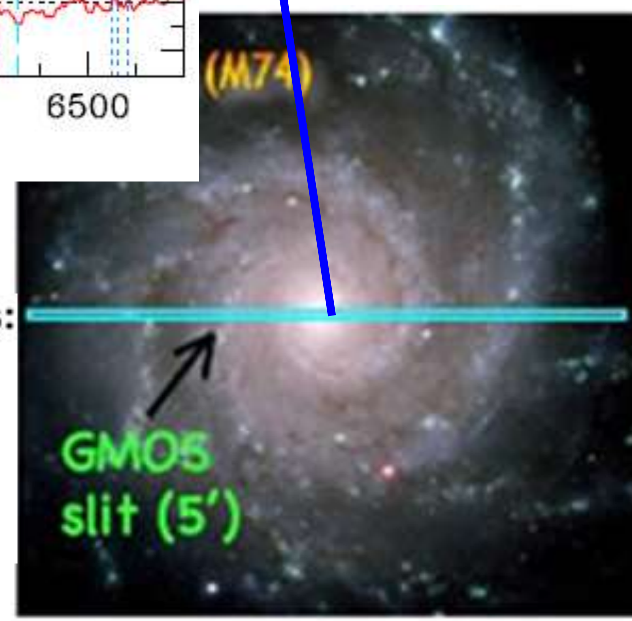

2009 MNRAS, 395, 28

Stellar Population and Kinematic Profiles In Spiral Bulges & Disks: Population Synthesis of Integrated Spectra

Lauren A. MacArthur[1]*, J. Jesús González[2]†, and Stéphane Courteau[3]‡
[1]*Department of Astrophysics, California Institute of Technology, MS 105-24, Pasadena, CA 91125*
[2]*Instituto de Astronomía, Universidad Nacional Autónoma de México, Apdo Postal 70-264, Cd. Universitaria, 04510 México*
[3]*Department of Physics, Engineering Physics & Astronomy, Queen's University, Kingston, ON K7L 3N6, Canada*

GMOS long-slit

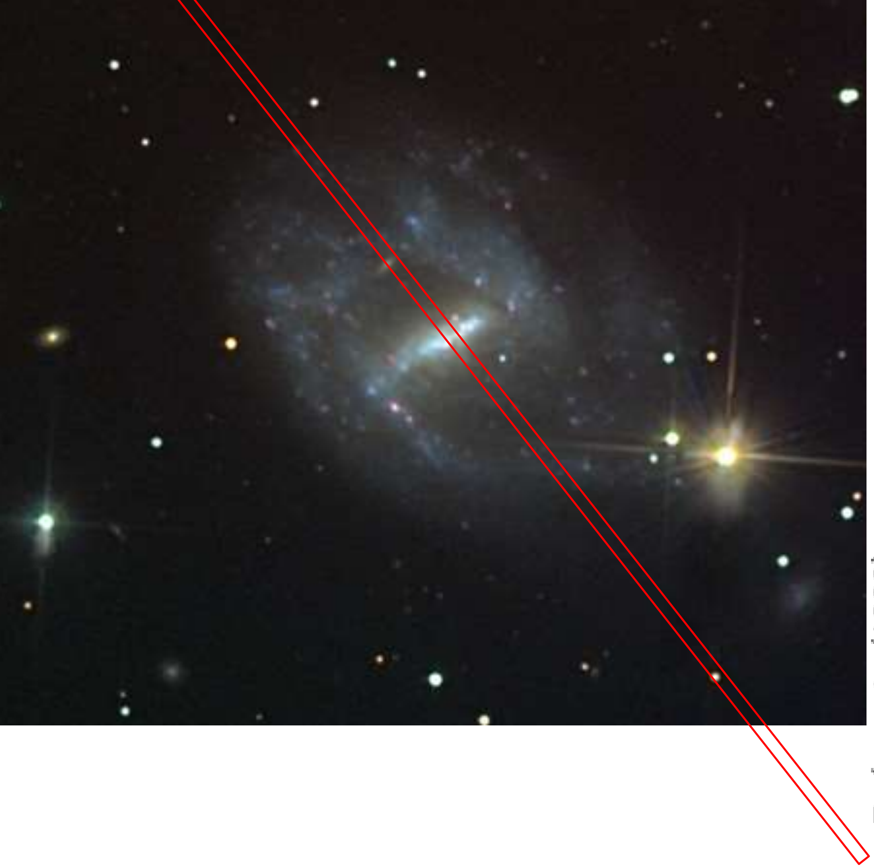

Spiral barred galaxy NGC 7741

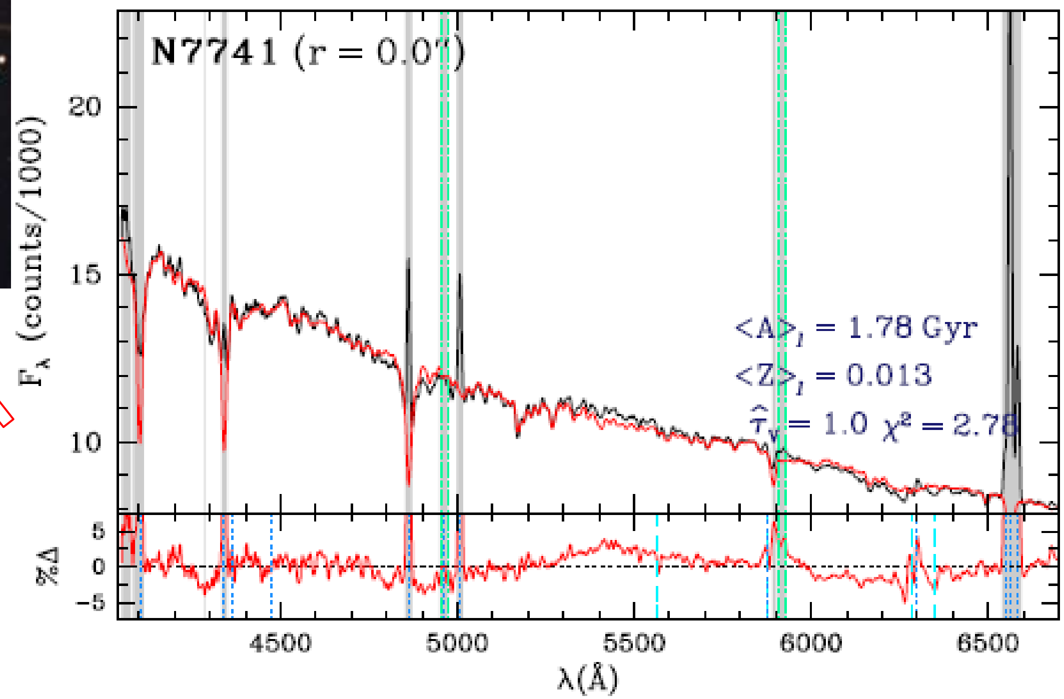

2009 MNRAS, 395, 28

Stellar Population and Kinematic Profiles In Spiral Bulges & Disks: Population Synthesis of Integrated Spectra

Lauren A. MacArthur[1]*, J. Jesús González[2]†, and Stéphane Courteau[3]‡

[1]*Department of Astrophysics, California Institute of Technology, MS 105-24, Pasadena, CA 91125*

[2]*Instituto de Astronomía, Universidad Nacional Autónoma de México, Apdo Postal 70-264, Cd. Universitaria, 04510 México*

[3]*Department of Physics, Engineering Physics & Astronomy, Queen's University, Kingston, ON K7L 3N6, Canada*

GMOS multislit

- With a 5.5 arcmin field of view, 30-60 slits can typically be located in a single mask
- maximum of several hundred slits when using narrow-band filters
- Slit widths 0.5 arcsec or larger
- Masks designed from GMOS direct imaging
- R (max) = 4000 ?

Object slits (white & yellow) with the alignment stars (cyan) , CCD gaps (blue) and the mask area (red) plotted over the GMOS pre-imaging. This plot is used to check the masks

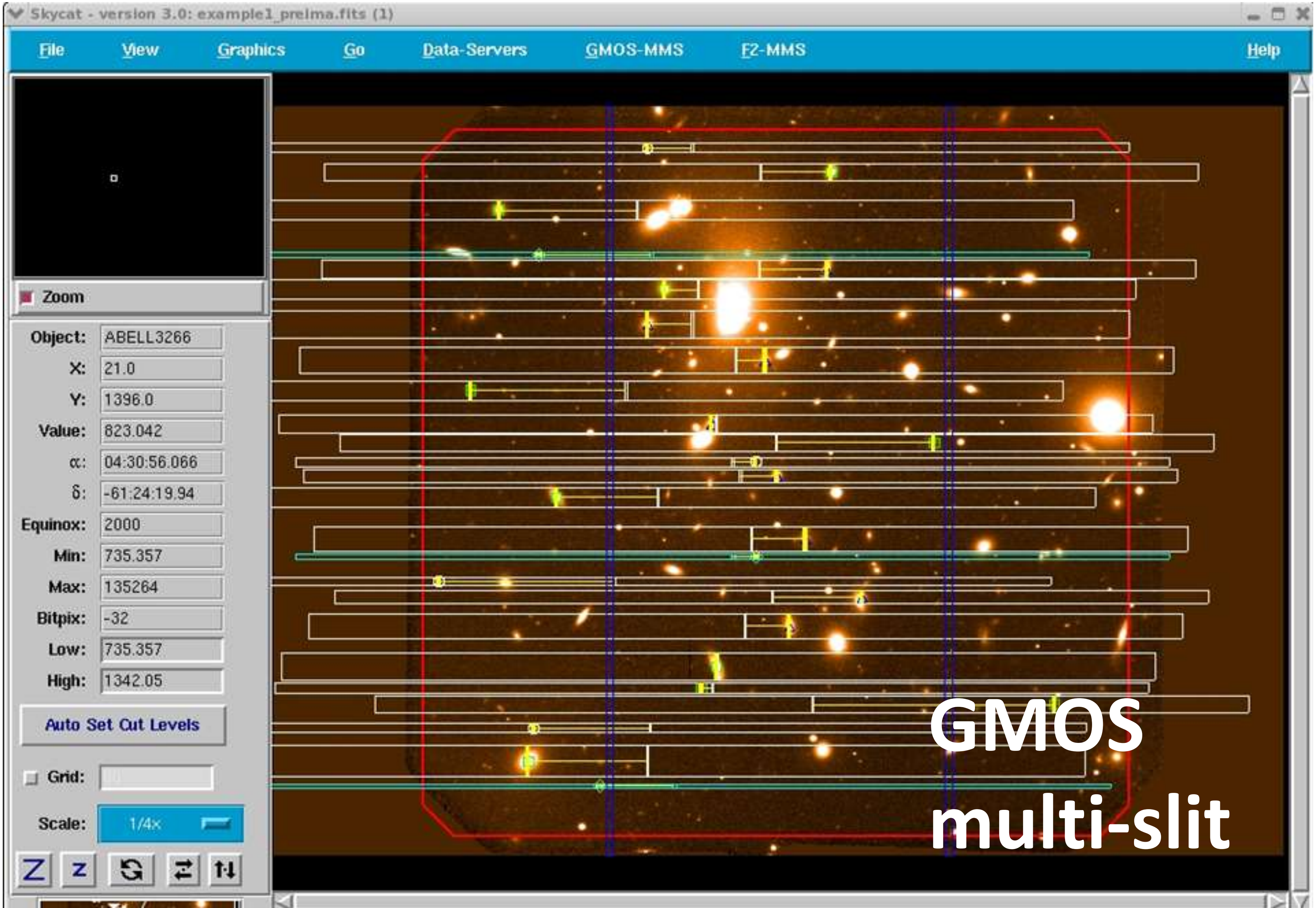

DEI**MOS** (Keck II)

DEep Imaging Multi-Object Spectrograph

DEIMOS Optical Layout

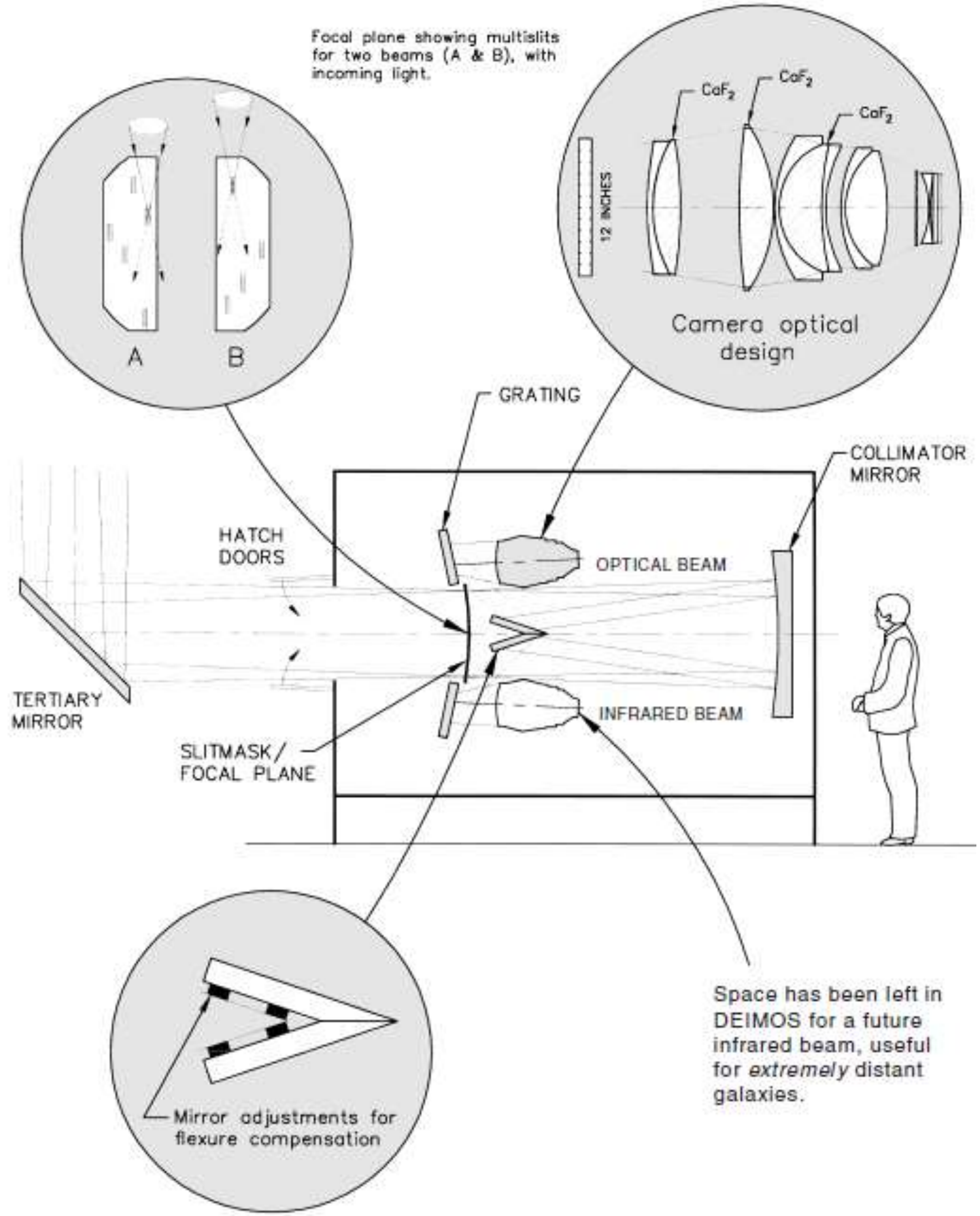

Enlargement of the Hubble Deep Field showing the faintest images of distant galaxies ever taken. Arrows pointing to galaxies show their redshifts—larger redshifts are more distant. The figure illustrates how images by themselves cannot tell distance; similar-looking galaxies in this picture have very different redshifts. The DEEP Survey will map redshifts on the sky with greater density than shown here, and over an area 15,000 times larger. The redshifts in this photo were made possible by the Keck telescope, the only telescope in the world capable of measuring such faint galaxies. (Courtesy: Space Telescope Science Institute.)

DEIMOS (Keck II)

- generous slit length spanning 16.6 arcmin on sky (vs. 5,5 arcmin for Gemini GMOS)
- large 8k×8k detector mosaic featuring eight CCDs
- advanced, closed-loop flexure compensation system achieving image stability of ±0.25 px over 360° of instrument rotation
- wide spectral coverage (up to 5000 Å per exposure)
- high spectral resolution (up to R≈6000)
- multi-slit spectroscopy of 100+ resolved targets per mask or 1000+ targets with narrow-band filters
- convenient IDL-based data reduction pipeline

Integral Field Spectroscopy (IFU)

Microlentes
+ fibras

fenda

Espectros
no detetor

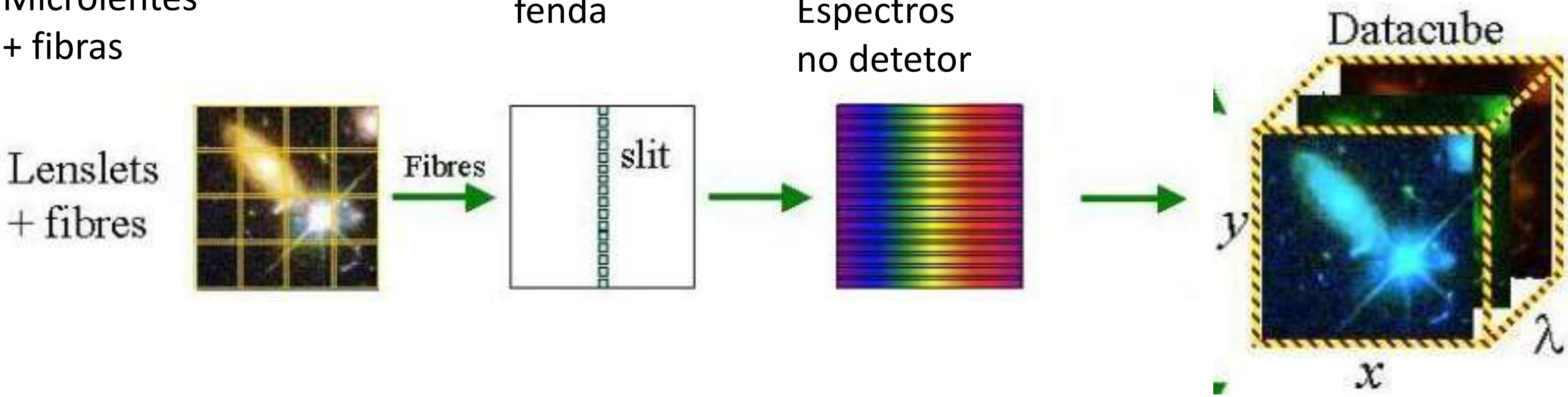

GMOS IFU

- Lenslet array (containing 1500 elements) in the pre-slit slice the focal plane into many components.
- Each lenslet is coupled to a fiber.
- The fibers end at the slit of the spectrograph.
- The science field of view is 35 square arcsec (5"x7") and is sampled by 1000 elements. The sky is sampled by the remaining 500 elements which are located ~1 arcmin away from the science field

University of Durham — *GMOS Integral Field Unit* observes NGC1068

Image taken by GMOS without using the IFU

The GMOS IFU records a spectrum for each pixel

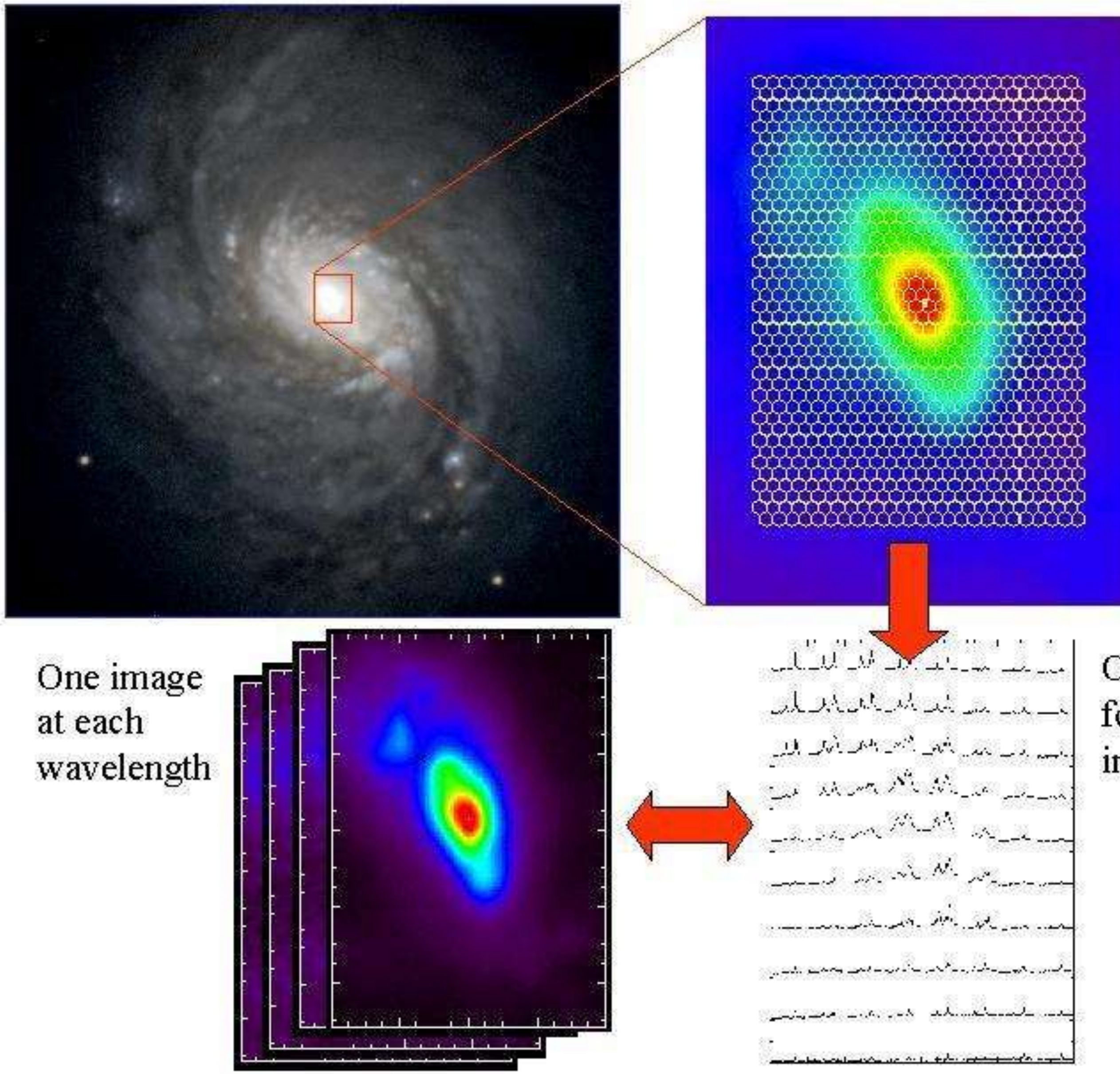

One image at each wavelength

One spectrum for each pixel in the image

Multi-object spectroscopy with fibers

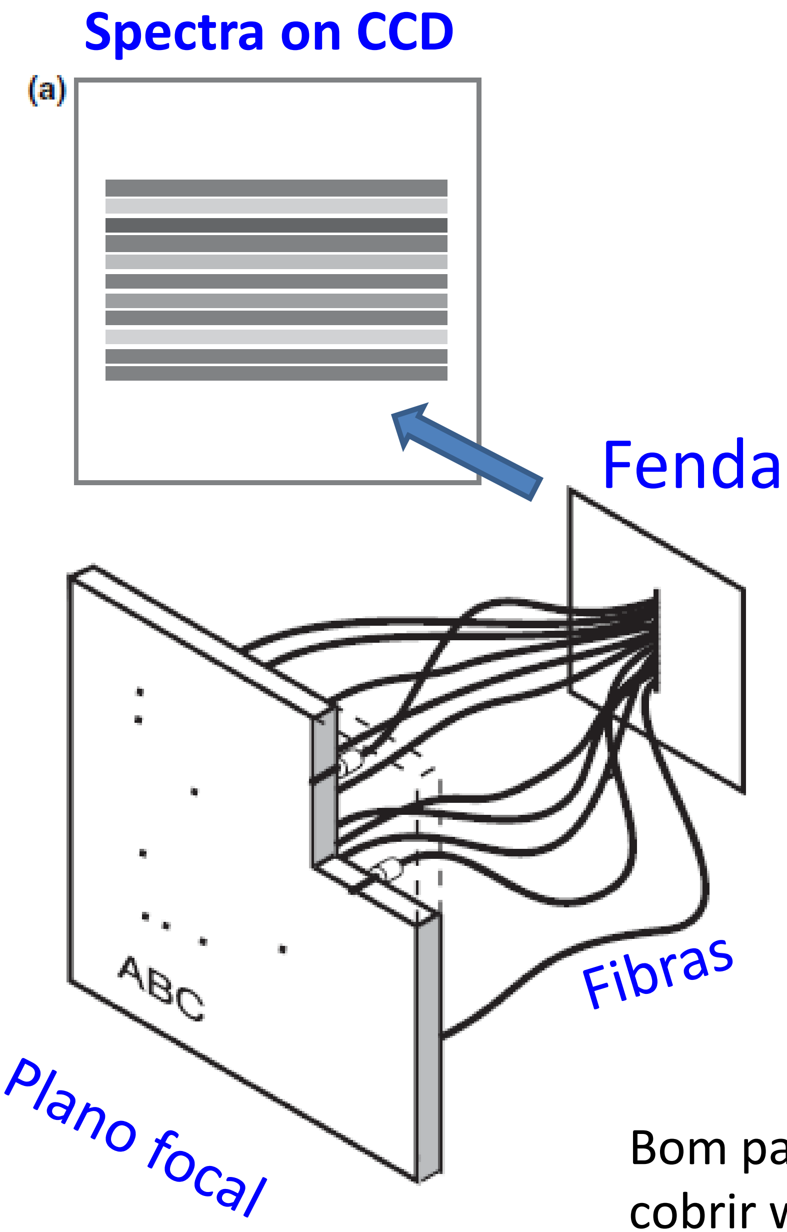

M80 globular cluster

Bom para objetos espaçados, permite cobrir wide fields

Fibras são posicionadas usando *magnetic buttons*

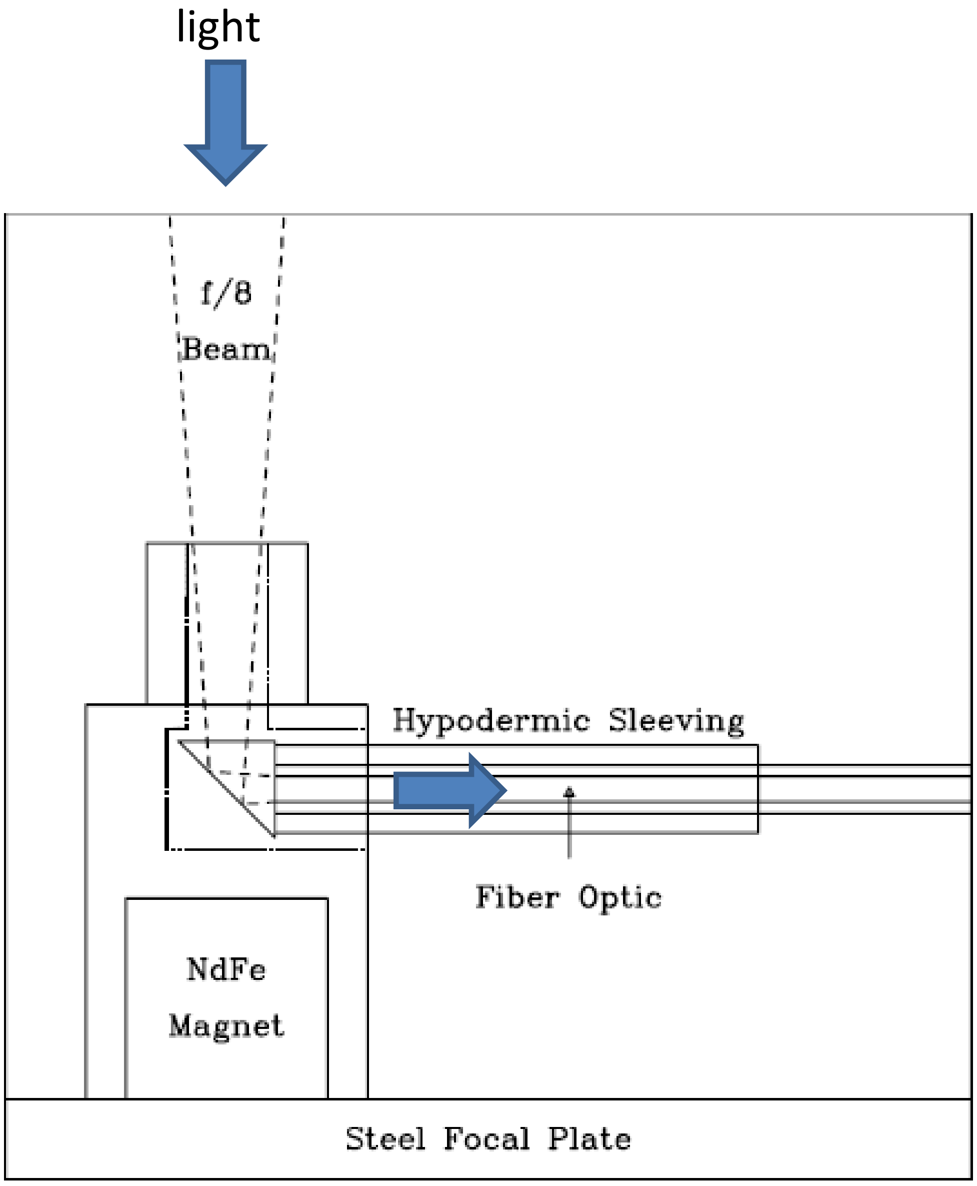

Figure 1: Schematic view of a fiber button on the focal plate

The 2dF robotic fibre positioner which feeds the AAOmega spectrograph is mounted at the *prime focus* on top of the AAT 3,9m telescope.

Spectrograph is at the coude room (38 m de fibras opticas)

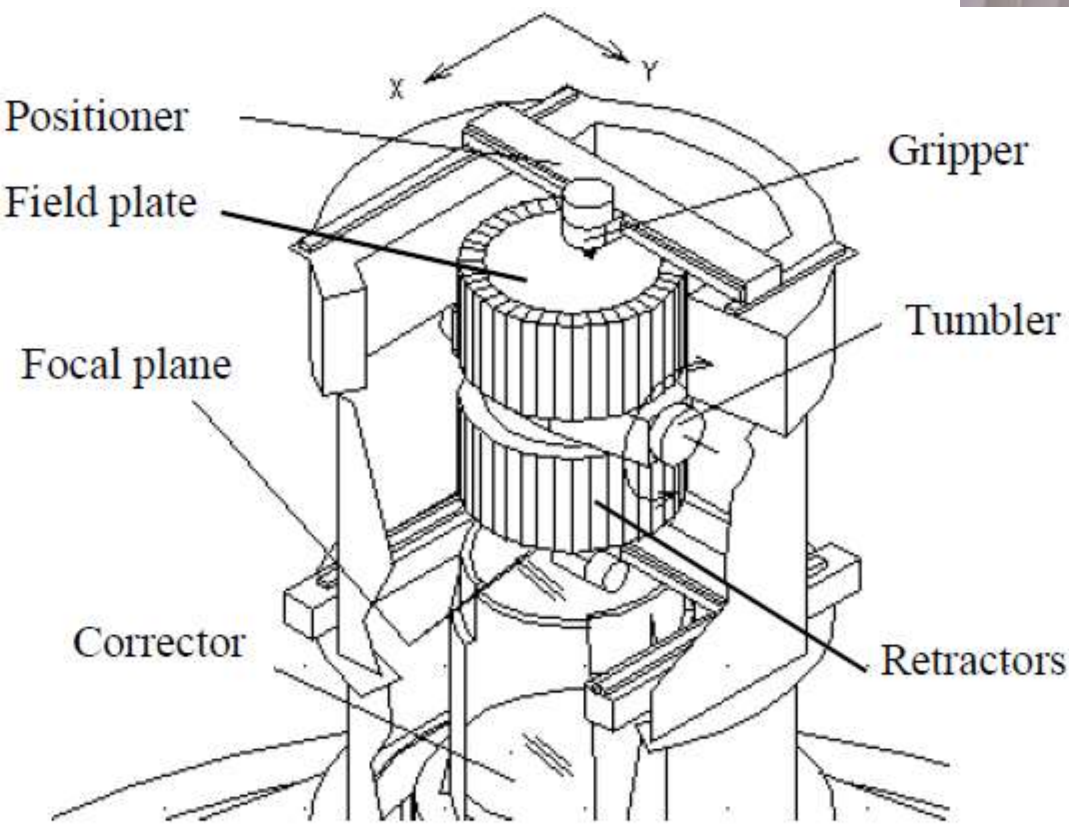

Figure 2 Cutaway view of 2dF postioner and plate exchanger

The 2dF robotic fibre positioner

The metal *field plate* is seen populated with *fibre buttons* which are used to relay the light from astronomical targets down to the AAOmega spectrograph. The *robot gripper* is seen hovering over a button which it is about to move to a new target position.

Old 2dF (one arm)
Almost 400 spectra (200 in each CCD)

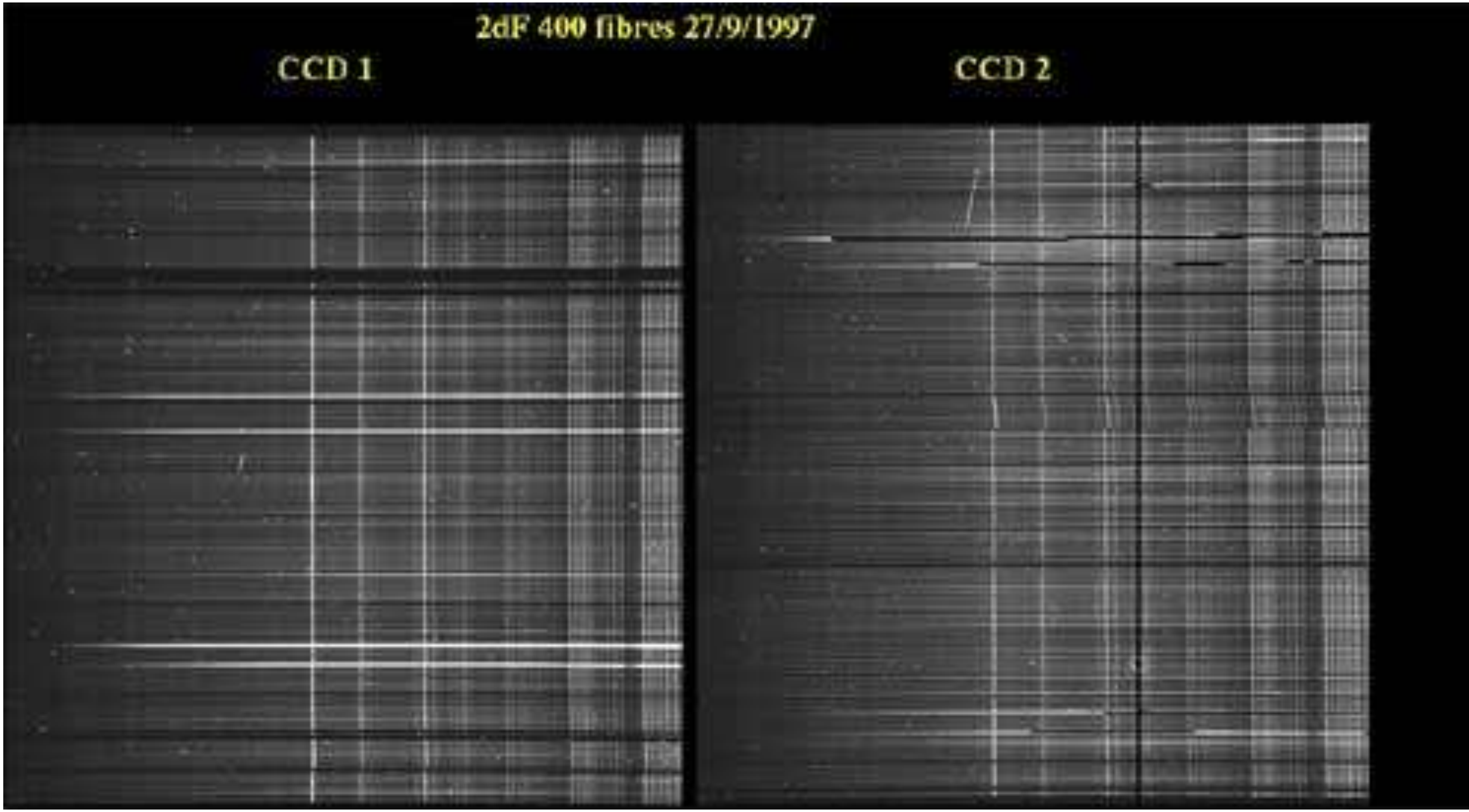

Latest 2dF AAOmega spectrograph (2005)

- 2 degree field of view (compare to 5 arcmin GMOS)
- About 400 fibers
- Two arms covering full optical range 370-850nm, or 470-950 nm at R ~ 1300
- Resolving power up to

R ~ 10 000 is possible but with smaller spectral coverage

- Simultaneous robotic

configuration for next field

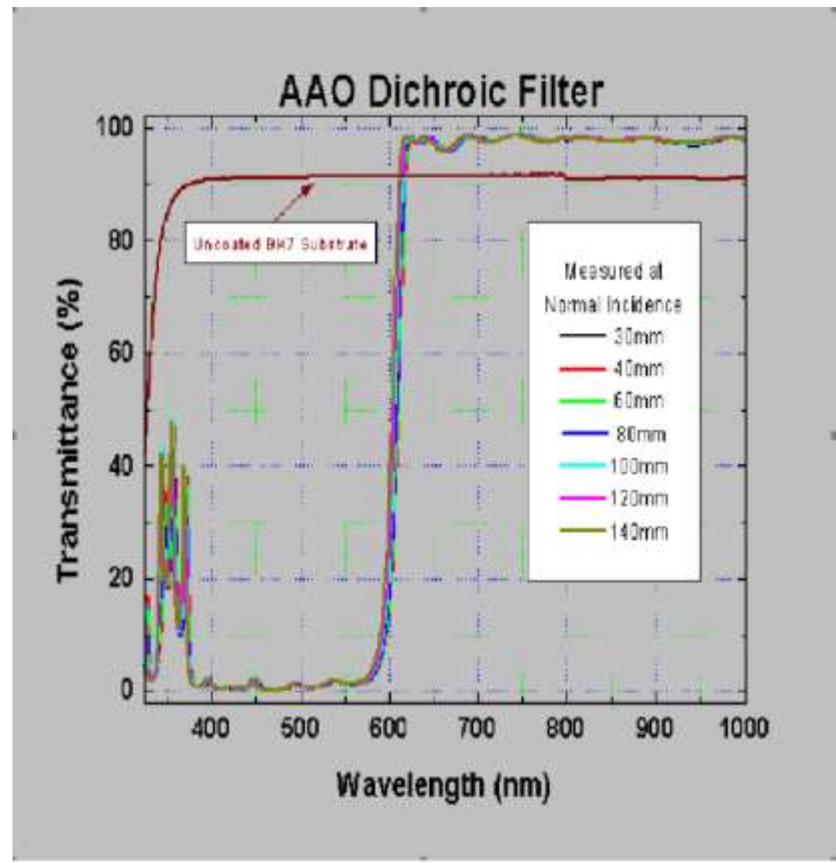

Almost 400 spectra for red arm (tem mais 400 espectros no lado azul)

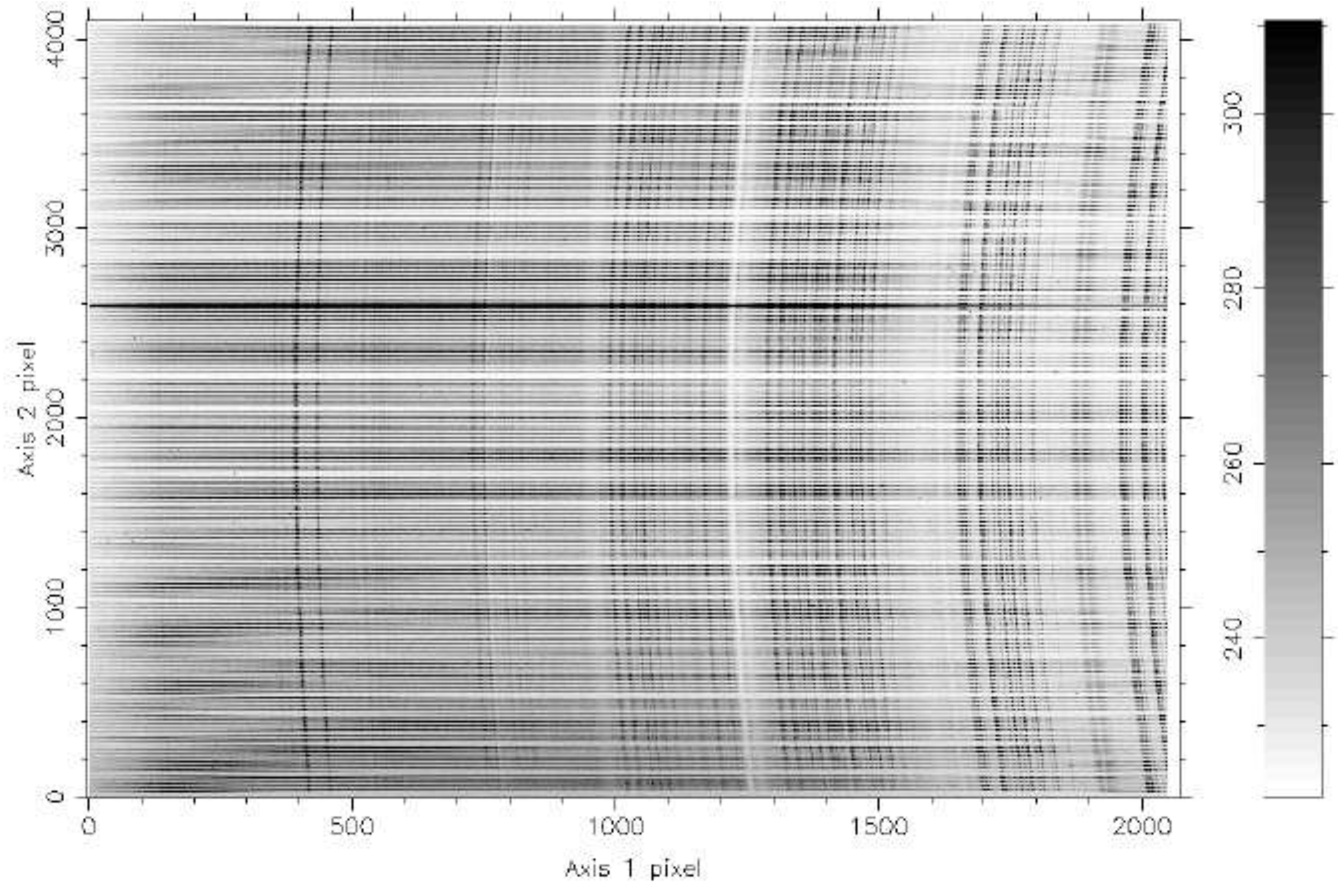

Figure 3. This 2hour (4×1800sec) raw AAOmega frame shows the full 2D CCD frame containing the 392 science fibre spectra. Dispersion runs left to right in the low resolution red (λ_{cen}=7250Å, R∼1300) unextracted spectra. Note the spectral curvature in the unsubtracted sky emission lines.

Sky subtraction with 2dF/AAOmega

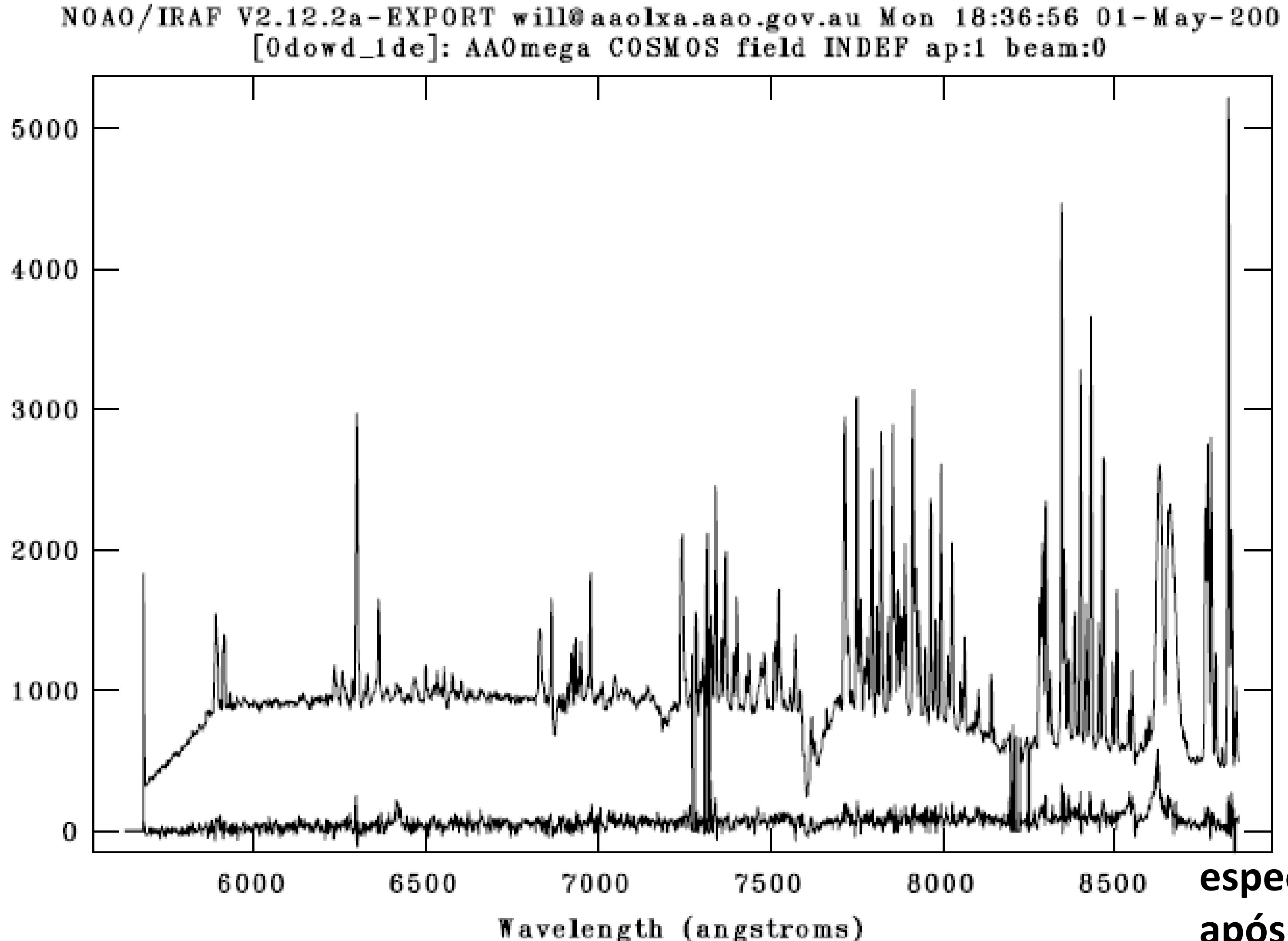

espectro do céu

espectro do quasar após subtração do céu

Figure 4. An example spectrum shows the ~1% sky subtraction which can be routinely achieved with AAOmega. The lower trace shows the spectrum of the underlying faint quasar target once the strong night sky spectrum (upper trace) has been subtracted. Bad pixel masking has not yet been full integrated into the reduction software, as evidenced by the two

Redução automática no 2dF AAOmega

400 blue spectra + 400 red spectra !

http://www.aao.gov.au/2df/aaomega/aaomega_2dfdr.html

Astronomy | Instrumentation | Observing | Images

2dfdr Software

`2dfdr` is an automatic data reduction pipeline dedicated to reducing multi-fibre spectroscopy data (with current implementations for AAOmega with either the 2dF or SPIRAL IFU top ends, 2dF, 6dF, FMOS and the older Spiral). A graphical user interface is provided to control data reduction and allow inspection of the reduced spectra. It is being continually developed at the AAO in response to user feedback. You **can** reduce most of your data by simply pressing **SETUP+START** in the Graphical User Interface.

An Efficient Approach to Obtaining Large Numbers of Distant Supernova Host Galaxy Redshifts

http://adsabs.harvard.edu/abs/2012arXiv1205.1306L

C. Lidman[A,B,Q], *V. Ruhlmann-Kleider*[C], *M. Sullivan*[D], *J. Myzska*[A,E], *P.*

Abstract: - We use the wide–field capabilities of the 2dF fibre positioner and the AAOmega spectrograph on the Anglo-Australian Telescope (AAT) to obtain redshifts of galaxies that hosted supernovae during the first three years of the Supernova Legacy Survey (SNLS). With exposure times ranging from 10 to 60 ksec per galaxy, we were able to obtain redshifts for 400 host galaxies in two SNLS fields, thereby substantially increasing the total number of SNLS supernovae with host galaxy redshifts. The median redshift of the galaxies in our sample that hosted photometrically classified Type Ia supernovae (SNe Ia) is $z \sim 0.77$, which is 25% higher than the median redshift of spectroscopically confirmed SNe Ia in the three–year sample of the SNLS. Our results demonstrate that

:rographs on 4m telescopes to efficiently

ost galaxies over the large areas of sky

nova surveys, such as the Dark Energy

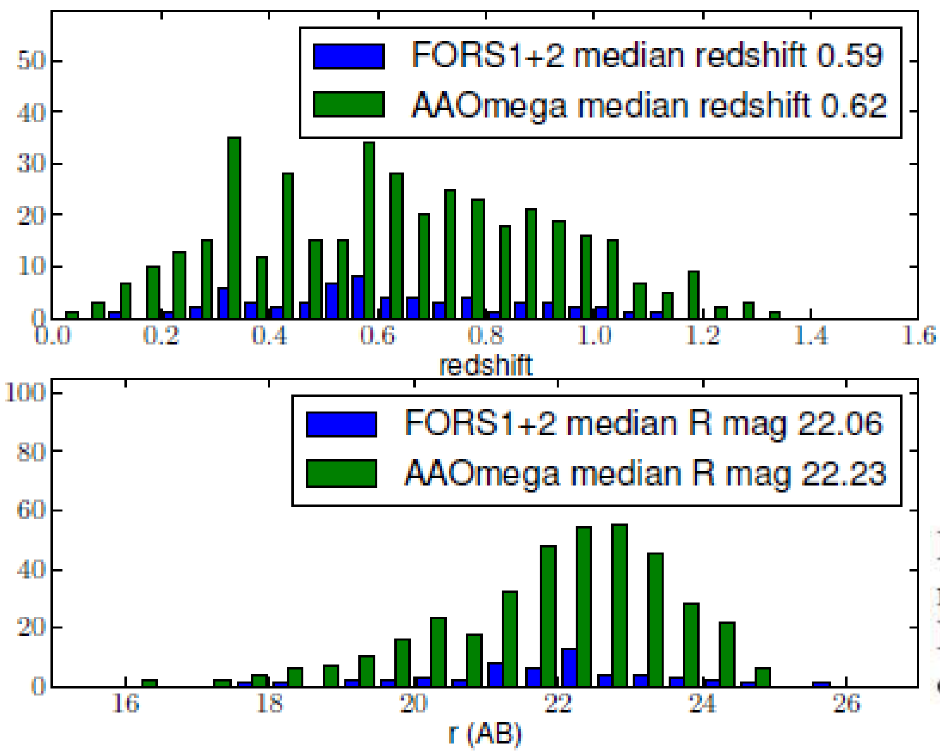

AAOmega no telescópio AAT de 4m é mais produtivo que o FORS no VLT de 8m (campo de apenas 7' x 7')

Figure 3: A comparison of the host redshift and magnitude distributions obtained with FORS1 and FORS2 with the host and magnitude distributions obtained with AAOmega.

Multi-object spectroscopy of stars in the CoRoT fields

II. The stellar population of the CoRoT fields IRa01, LRa01, LRa02, and LRa06⋆,⋆⋆

E. W. Guenther[1], D. Gandolfi[2], D. Sebastian[1], M. Deleuil[3], C. Moutou[3], and F. Cusano[4]

A&A 543, A125 (2012)

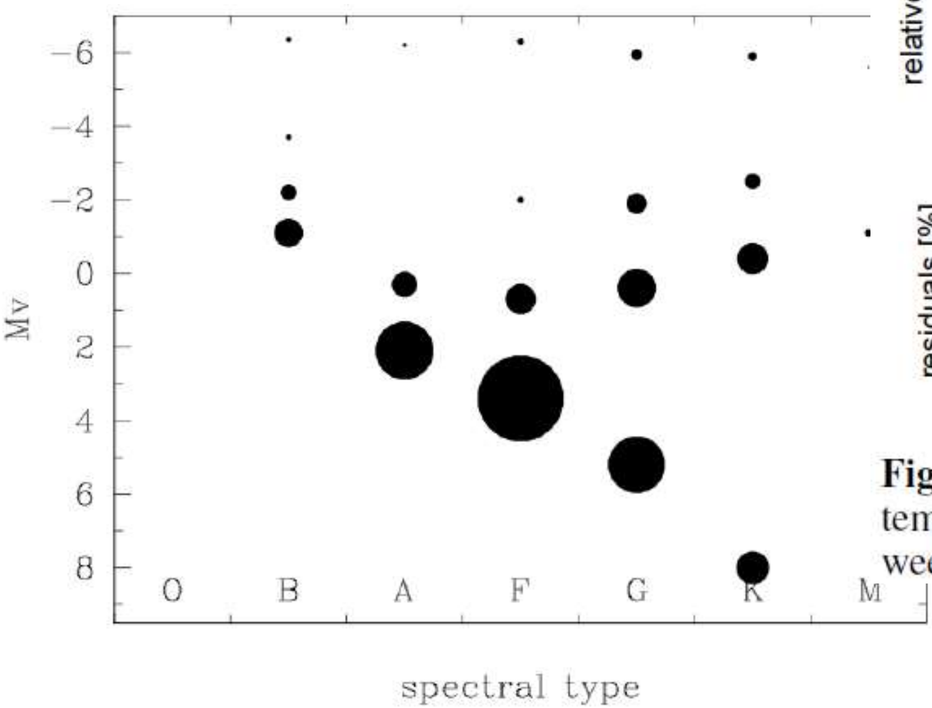

Fig. 4. HRD of the stars observed by CoRoT. The size of the circles is proportional to the number of stars of that category.

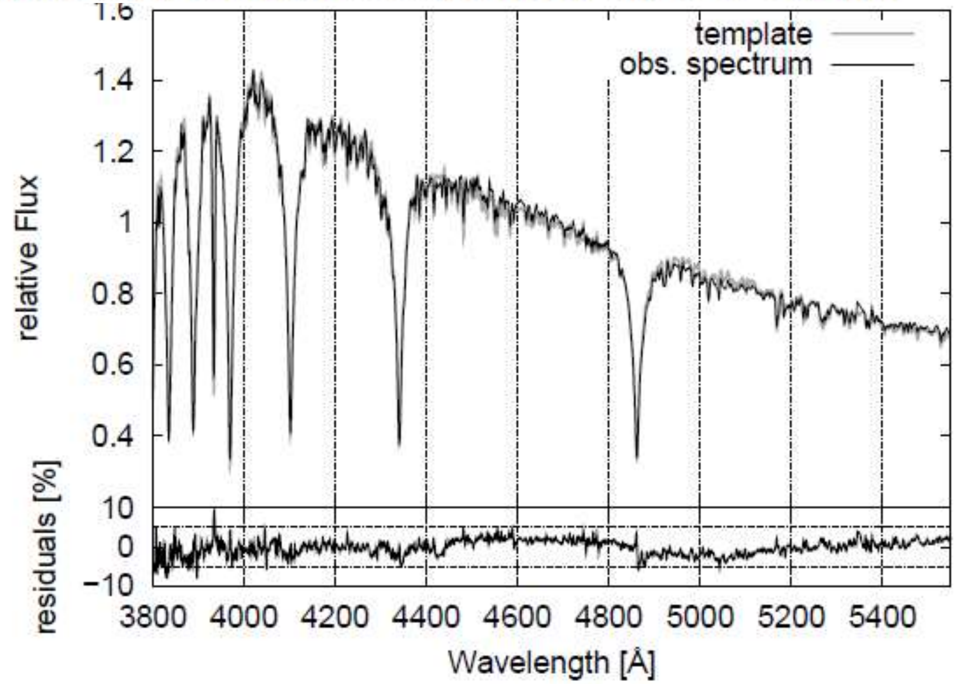

Fig. 5. Spectrum of an A5V-star (black line), together with the template (grey line). The lower panel shows the residuals between the two spectra.

	T_{eff}	log *g*	[Fe/H]
Candidate Sun (2df):	5783,	4.41,	0.08
Subaru spectra:	5822,	4.31,	0.09

Mon. Not. R. Astron. Soc. **411**, 1536–1546 (2011)

Radial velocity and metallicity of the globular cluster IC4499 obtained with AAOmega*

Warren J. Hankey† and Andrew A. Cole

School of Mathematics & Physics, University of Tasmania, Private Bag 37, Hobart TAS 7001, Australia

The half-light and tidal radii of IC 4499 are 1.5 and 12.35 arcmin, respectively (Harris 1996). Fibres were preferentially allocated to the centre of the 2° field. Once the cluster centre was sampled as densely as possible with fibres, the spare fibres were allocated to stars outside the cluster centre in the same colour and magnitude

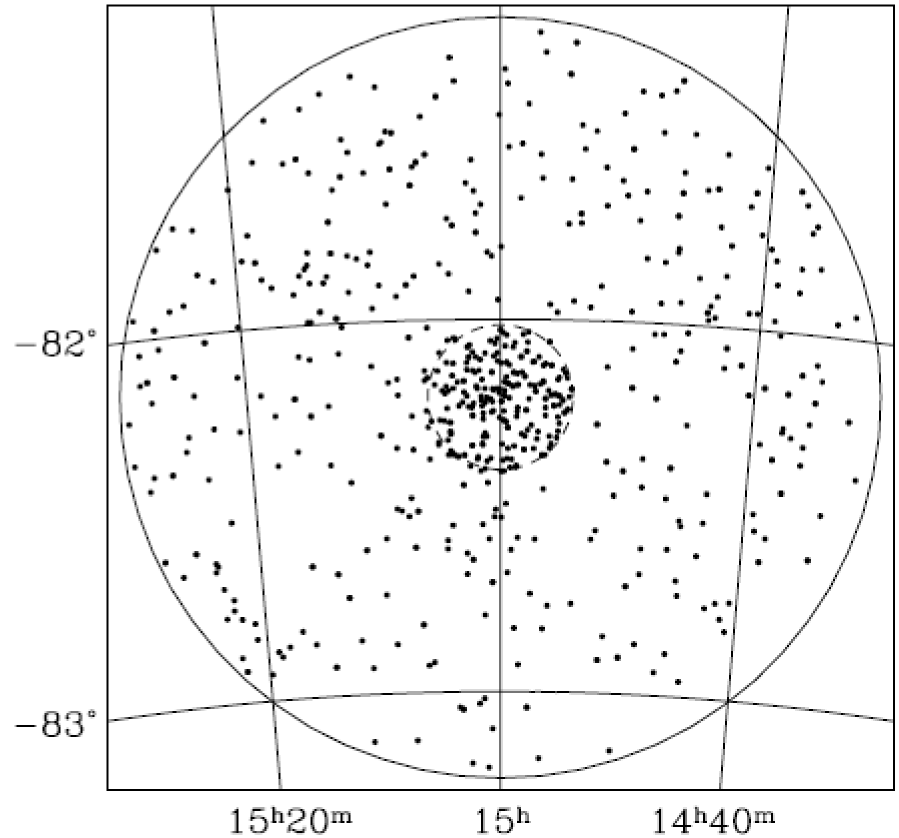

ɟure 2. Observed targets in a 2° field around IC 4499. The tidal radius shown by the dashed line; the fibre allocation was strongly weighted to ect targets within this radius.

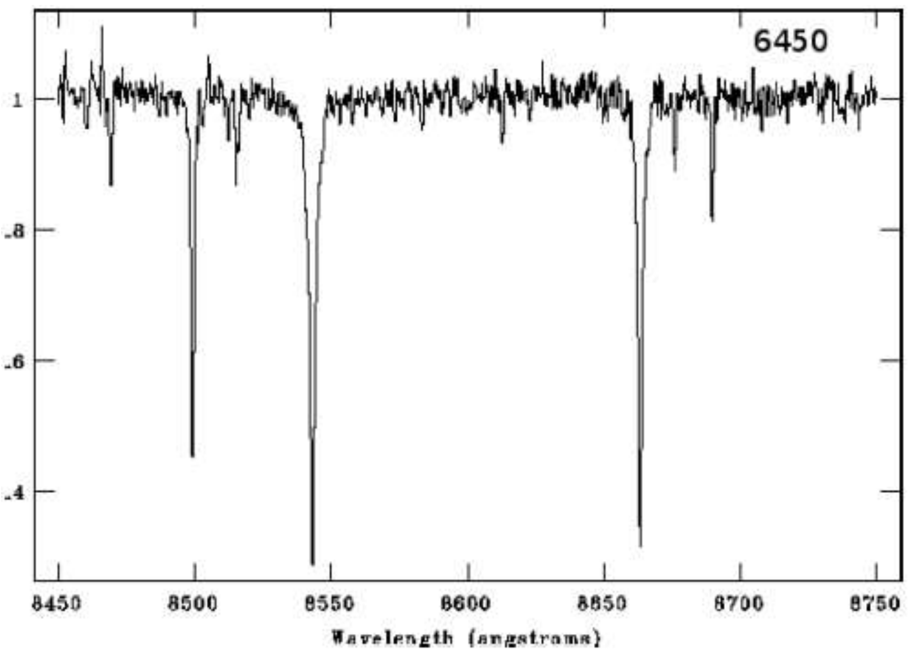

Figure 3. Typical spectrum of IC 4499 member RGB star showing the Ca II triplet and many weaker metal lines. Star ID 6450 in Table 3.

Confirmed members of cluster IC 4499

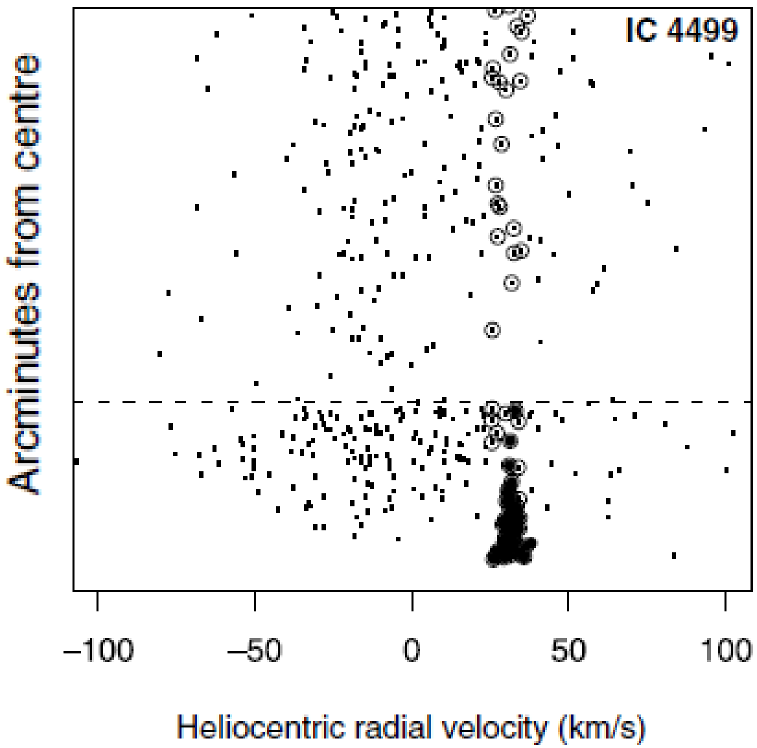

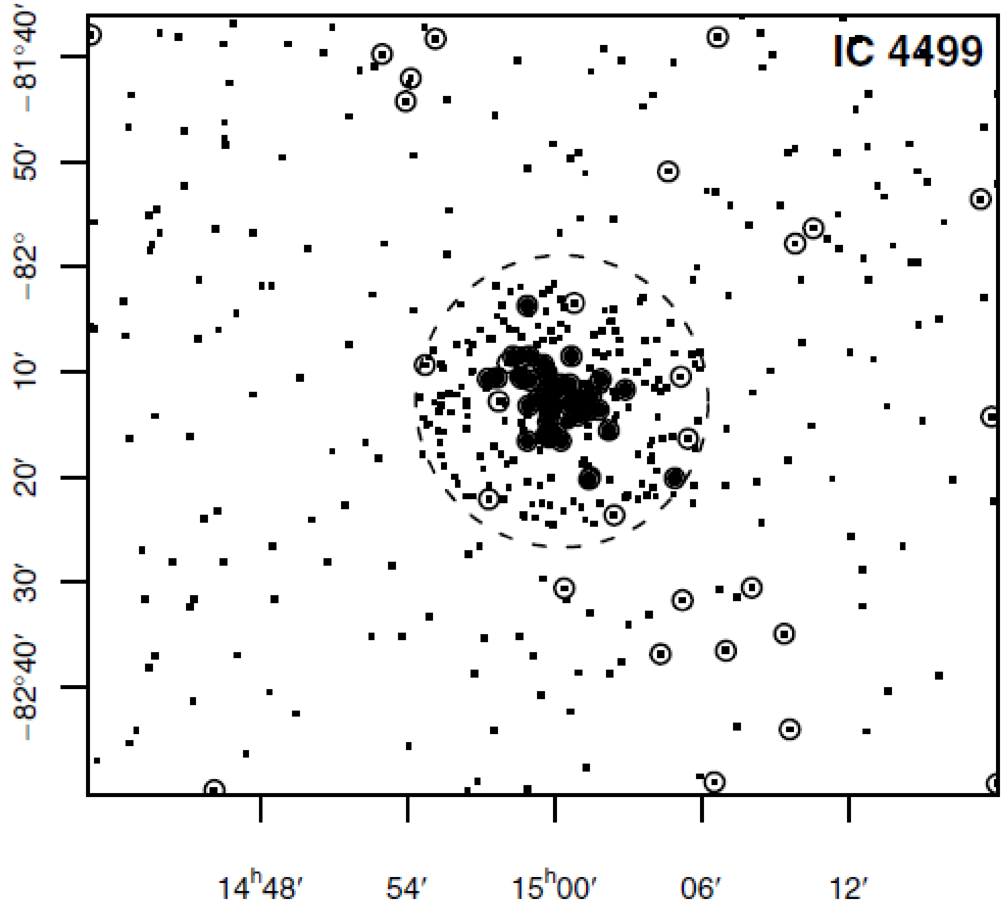

Figure 5. Cluster member map. Solid circles are cluster members. Open circles with similar velocities were rejected for lying outside the tidal radius (dashed line), as metallicity outliers, or for contaminated spectra.

Table 2. Summary of results.

Cluster	$N_\star$	W' (Å)	K_{HB} (mag)	[Fe/H]	Δ[Fe/H]	V_r (km s^{-1})	ΔV_r (km s^{-1})
M68	51	2.59 ± 0.35	14.4[a]	-1.88 ± 0.13	0.11 ± 0.14	-98.6 ± 1.5	-4.2 ± 4.2
M4	70	4.90 ± 0.34	11.13	-1.12 ± 0.14	0.07 ± 0.14	65.7 ± 0.9	5.2 ± 1.1
M22	81	3.61 ± 0.46	12.21	-1.55 ± 0.17	-0.07 ± 0.17	-150.5 ± 1.3	-1.7 ± 1.5
IC 4499	43	3.70 ± 0.29	15.97	-1.52 ± 0.12		31.5 ± 0.4	

[a] Dall'Ora et al. (2006). Δ is difference of measured − literature value.

Multi-fibre optical spectroscopy of low-mass stars and brown dwarfs in Upper Scorpius⋆,⋆⋆,⋆⋆⋆

A&A 527, A24 (2011)

N. Lodieu[1,2], P. D. Dobbie[3], and N. C. Hambly[4]

Context. Knowledge of the mass function in open clusters constitutes
posed to explain the existence of low-mass stars and brown dwarfs.
Aims. The aim of the project is to determine as accurately as possib
boundary in the young (5 Myr) and nearby (d = 145 pc) Upper Sco as
Methods. We have obtained multi-fibre intermediate-resolution (R ~ 1
and proper motion selected low-mass star and brown dwarf candidates
Australian Telescope.
Results. We have estimated the spectral types and measured the equiva
features to confirm the spectroscopic membership of about 95% of t
6.5 square degrees surveyed in Upper Sco by the UKIRT Infrared Dee
also detect lithium in the spectra with the highest signal-to-noise, con

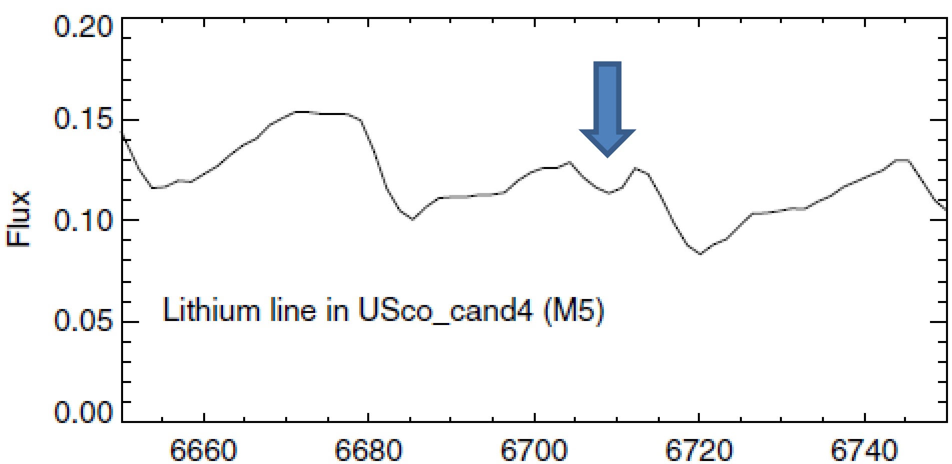

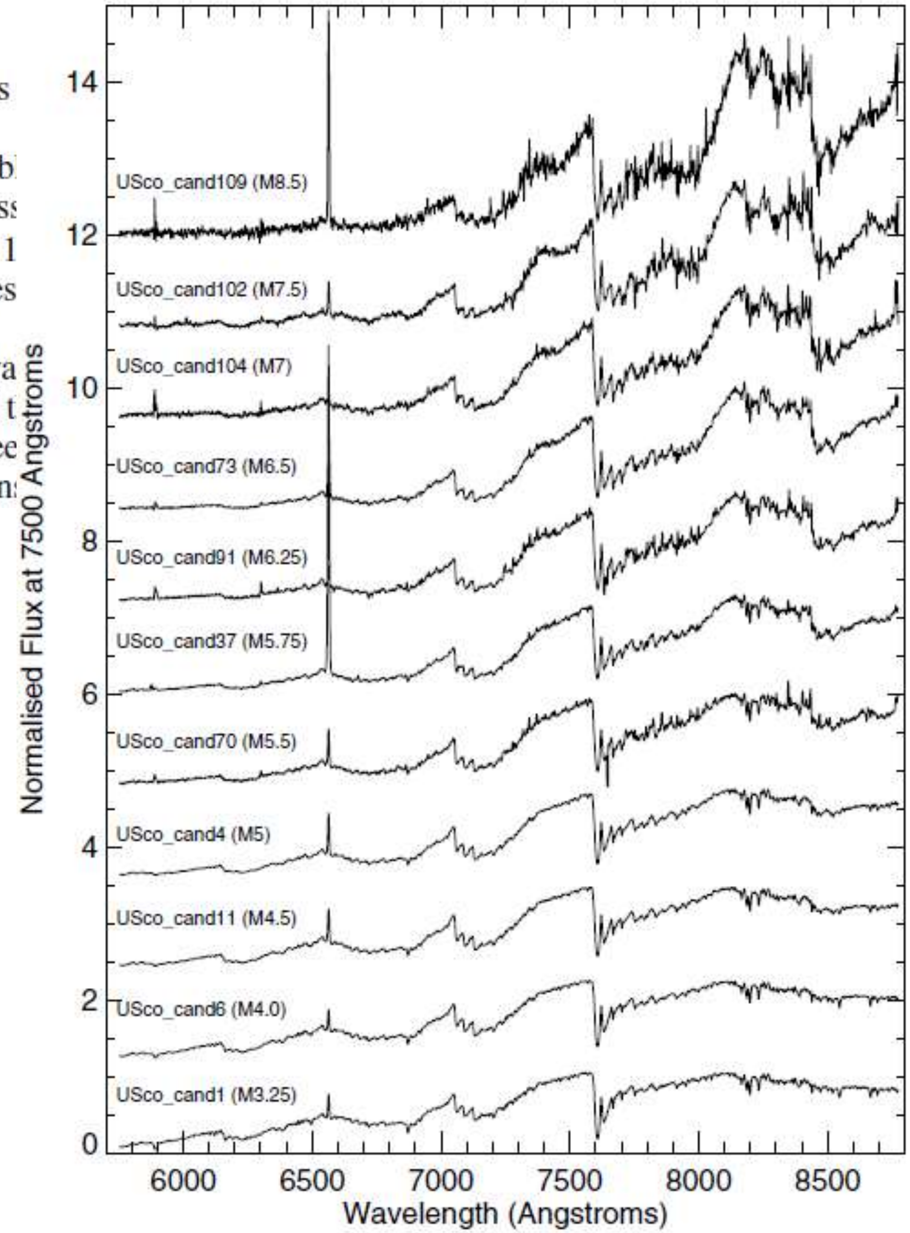

FLAMES (VLT/ESO) - Fibre Large Array Multi Element Spectrograph

- Field of view: 25 arcmin in diameter
- UVES mode is for high resolution

(R ~ 47 000) but only 8 objects

- GIRAFFE mode :

- MEDUSA submode up to 130 targets at R ~ 5600 - 25000

- IFU submode in small field 2x3arcsec

- ARGUS submode : larger IFU (12x7")

- Simultaneous UVES + GIRAFFE ok
- Pipeline (automatic data reduction)

Posicionamento das fibras no FLAMES

(em menos de 15 min enquanto são feitas observações em outra placa)

The Fiber Positioner (OzPoz)

The OzPoz fibre positioner is based on the successful concept developed for 2dF at AAO: while one plate is observing, the other one is positioning the fibres for the subsequent observations. The dead time between two observations is therefore limited to less than 15 minutes, guaranteeing a very good night duty cycle. OzPoz has the capability to host up to 560 fibre per plate.

OzPoz is able to host up to four plates, but only two are used in the FLAMES configuration. Each of these two plates will feed GIRAFFE and the red arm of the UVES spectrographs.

Plate One is hosting

- **132 GIRAFFE MEDUSA buttons,**
- **30 GIRAFFE IFU buttons (15 objects plus 15 sky),**
- **8 UVES buttons.**

With Plate One it is possible to use UVES and GIRAFFE simultaneously.
Plate Two is hosting

- **the same buttons as above,**
- **a central GIRAFFE IFU ``Argus" facility and 15 Argus-sky buttons.**

To these two plates, several buttons for centering and maintenance purposes have been added.
The **minimum object separation is 10.5 arcsec**. This minimum distance is entirely limited by the size of the magnetic buttons. OzPoz is able to position the fibres with an accuracy of better than **0.1 arcsec** (+ astrometric error). It has its own Observing Software and control electronics, as well as the necessary preparatory observing tools. Finally OzPoz is equipped with its own calibration system.

Very accurate calibrations can be obtained by rastering the fibre buttons with an r-theta arm, and repeating this procedure many times. Such calibrations are the only ones planned on a daily basis.

The Fibre Positioner (see ESO press realease 07-98) is being built by the AUSTRALIS Consortium, lead by the Anglo Australian Observatory (AAO, P.I. K. Taylor, Co-P.I. M. Colless).

Further information about OzPoz can be obtained here.

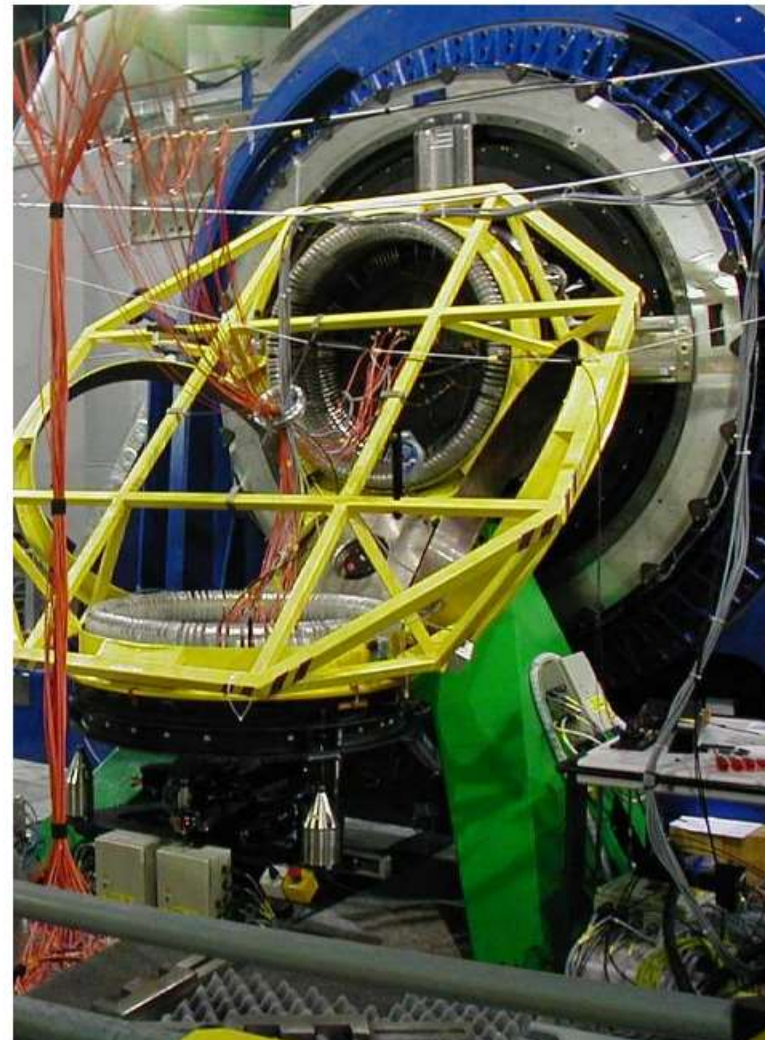

FLAMES/Giraffe spectrograph with Ozpoz

http://www.eso.org/sci/facilities/paranal/instruments/flames/inst/Giraffe.html

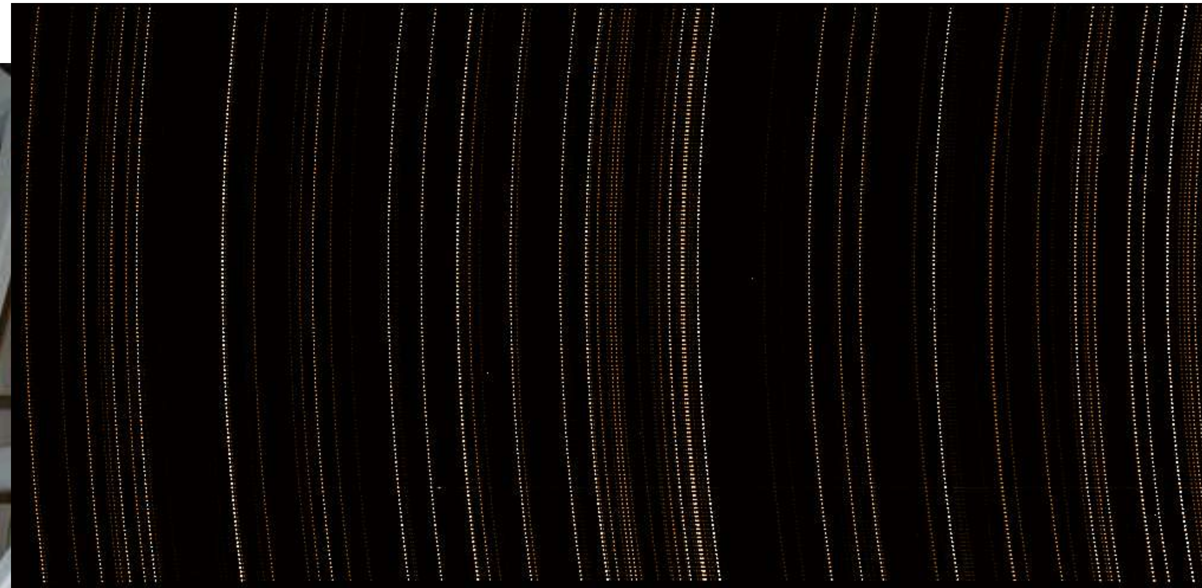

Th-Ar calibration in medusa mode using the HR9 setup. Lambda increases from right to left. The Y- axis gives the position along the slit

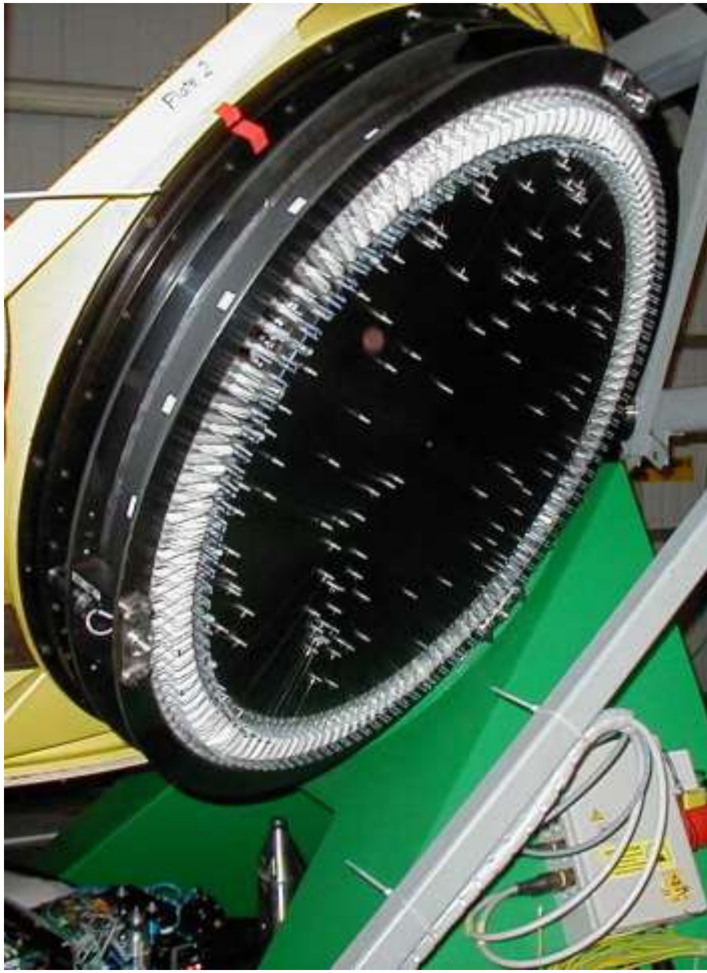

View of the back of one Ozpoz plate where all the fibres are attached with magnetic buttons

Flat-field image in medusa mode with the same HR9 setup. Wavelenghts are increasing from right to left. The vertical axis gives the position along the slit.

VLT/FLAMES spectroscopy of Red Giant Branch stars in the Carina dwarf spheroidal galaxy.*

B. Lemasle[1], V. Hill[2], E.Tolstoy[1], K. A. Venn[3], M. D. Shetrone[4], M. J. Irwin[5], T. J. L. de Boer[1], E. Starkenburg[1], and S. Salvadori[1]

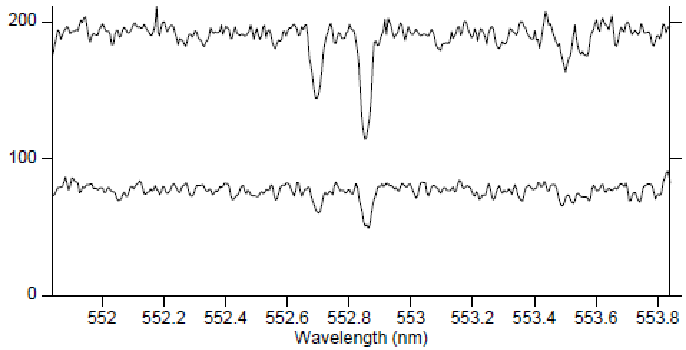

Fig. 1. Representative spectra of two stars of our sample, centered on the Mg line at 552.841 nm. *(top)* MKV0900: S/N=44, Vmag=17.79; *(bottom)* MKV0614: S/N=22, Vmag=18.72. A

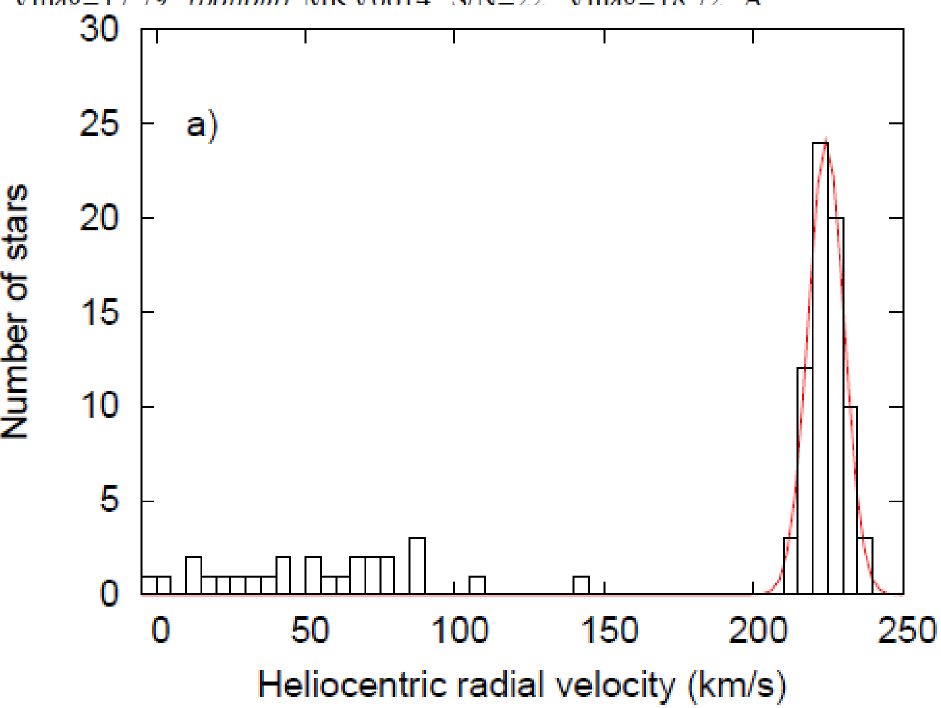

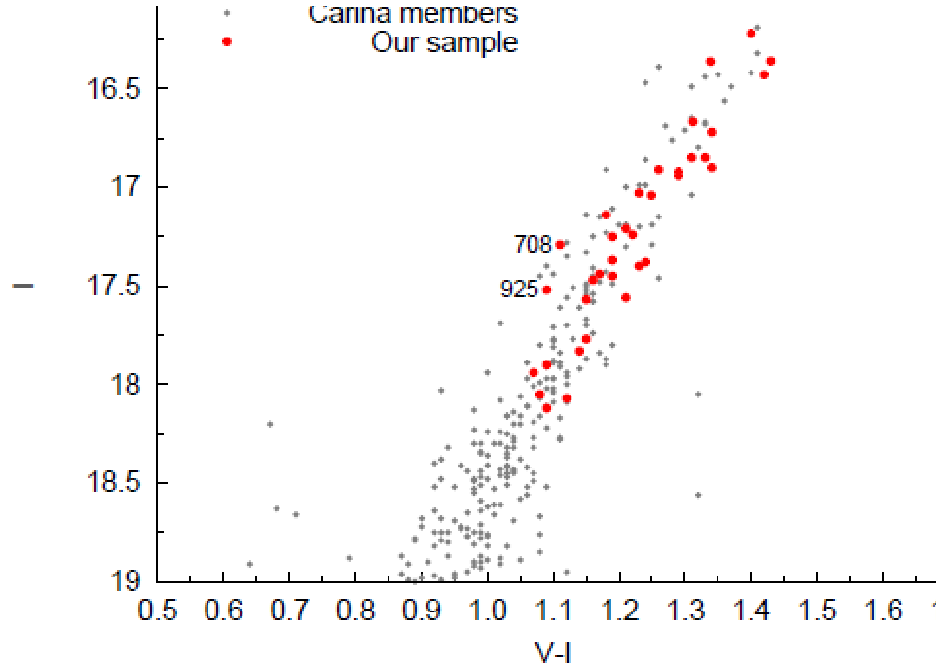

.3. I vs. (V-I) CMD: our FLAMES/GIRAFFE sample is wn in red dots and other Carina members (from CaT) are wn in grey dots.

2012A&A...538A.100L

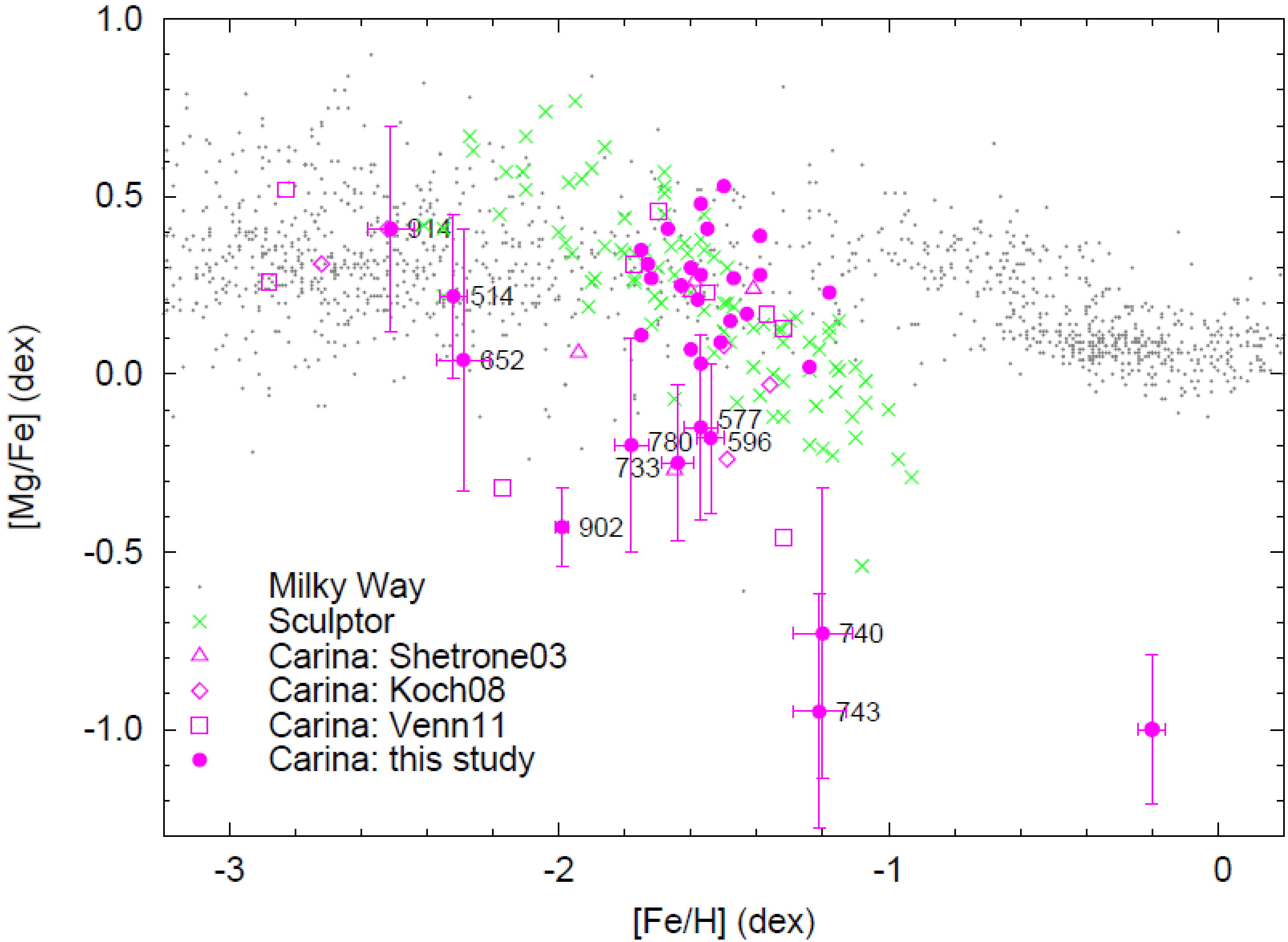

Fig. 7. The distribution of [Mg/Fe] for our sample of RGB stars in the Carina dSph as pink filled circles. Also included in the plot are the 5 RGB stars in the Carina dSph from Shetrone et al. (2003): pink open triangles; the 9 RGB stars from Venn et al. (2011): pink open squares and 6 of the RGB stars from Koch et al. (2008): pink open diamonds. Stars in Sculptor are in green crosses (Shetrone et al., 2003; Geisler et al., 2005; Hill et al., 2011). Milky Way halo stars are in small grey dots (from Venn et al. (2004) and references therein). Individual error bars are given for some peculiar stars and a representative error bar for the rest is given in bottom right hand corner.

Na-O anticorrelation and horizontal branches

II. The Na-O anticorrelation in the globular cluster NGC 6752

A&A 464, 927–937 (2007)

E. Carretta[1], A. Bragaglia[1], R. G. Gratton[2], S. Lucatello[2], and Y. Momany[2]

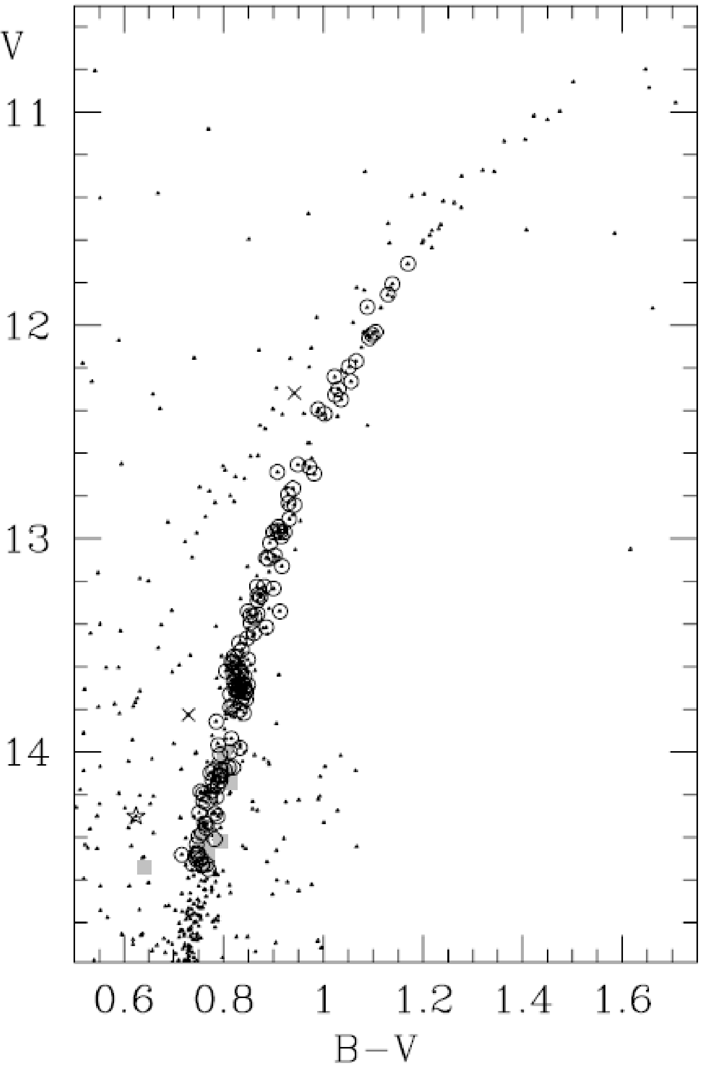

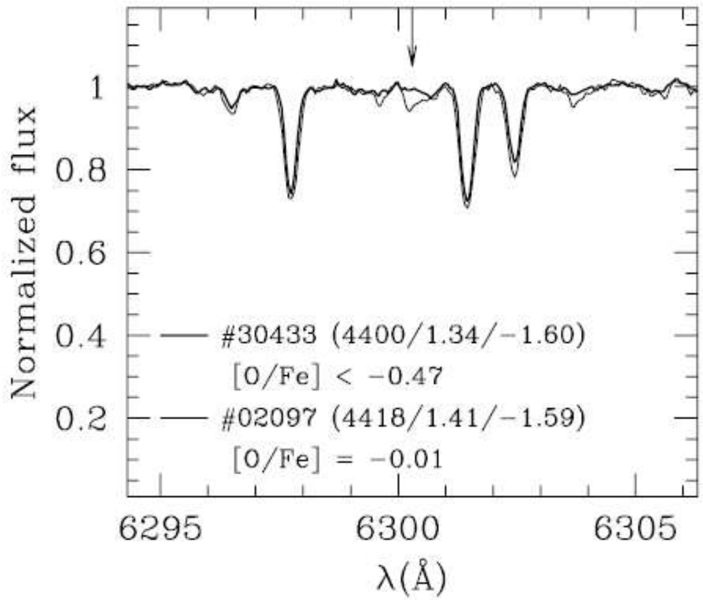

Fig. 6. Comparison of the observed spectra of stars 30433 and 2097 in NGC 6752 near the [O I] 6300.31 Å line. These stars have very similar atmospheric parameters ($T_{\rm eff}$, $\log g$ and [Fe/H] are indicated), yet quite different [O/Fe] abundances.

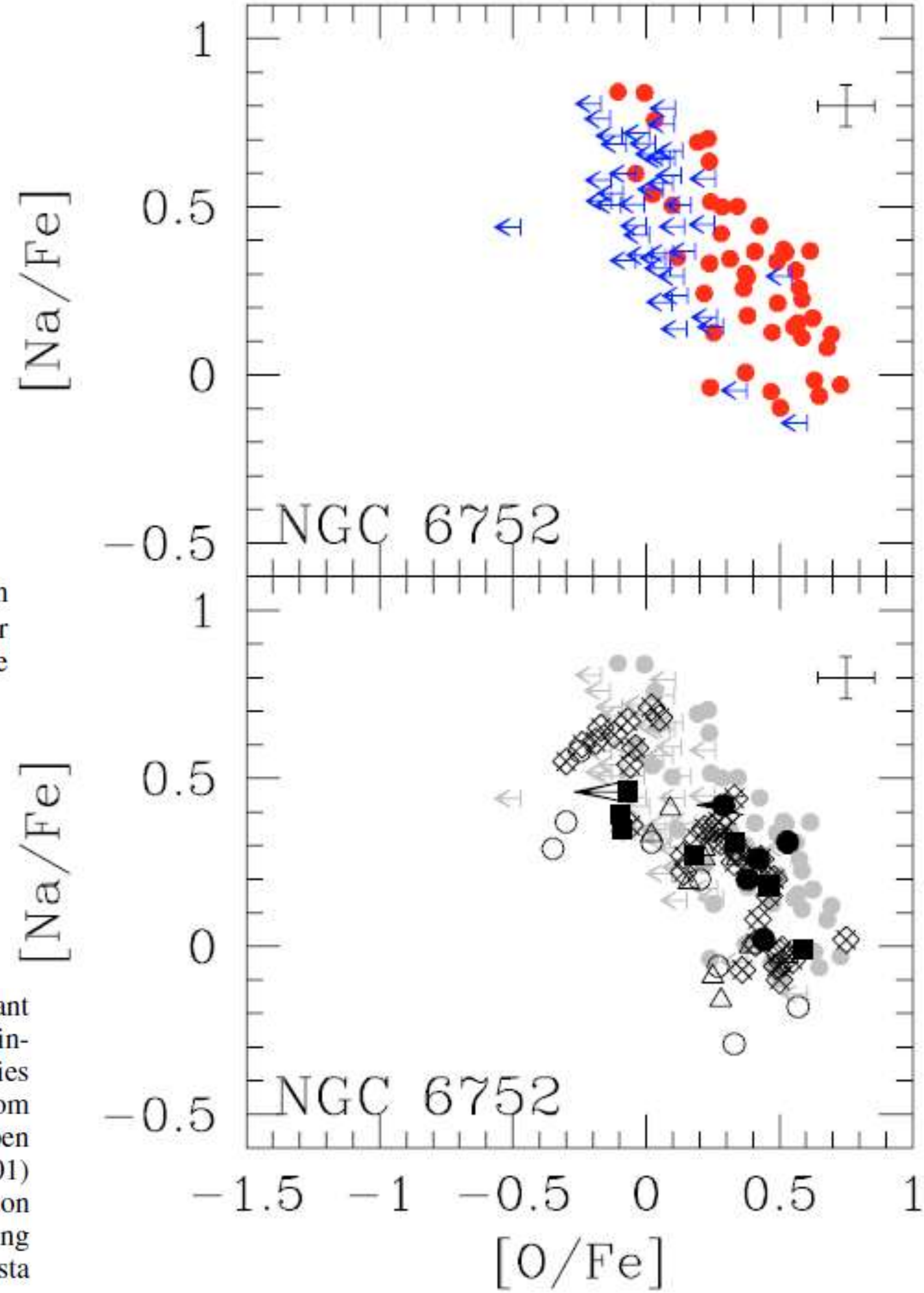

Fig. 5. *Upper panel*: [Na/Fe] ratio as a function of [O/Fe] for red giant stars in NGC 6752 from the present study. Upper limits in [O/Fe] are indicated as blue arrows. The error bars take into account the uncertainties in atmospheric parameters and *EW*s. *Lower panel*: literature data from several study (see text) superimposed to our results. Filled and open large circles are subgiant and turnoff stars from Gratton et al. (2001) and Carretta et al. (2004). Filled squares are RGB stars from Gratton et al. (2005). Diamonds with crosses inside are RGB stars from Yong et al. (2003, 2005). Open triangles are giants from Norris & Da Costa (1995) and Carretta (1994).

Deciphering the star-formation scenario of the Sh2-296 nebula. Profa. Jane + Beatriz Fernandes

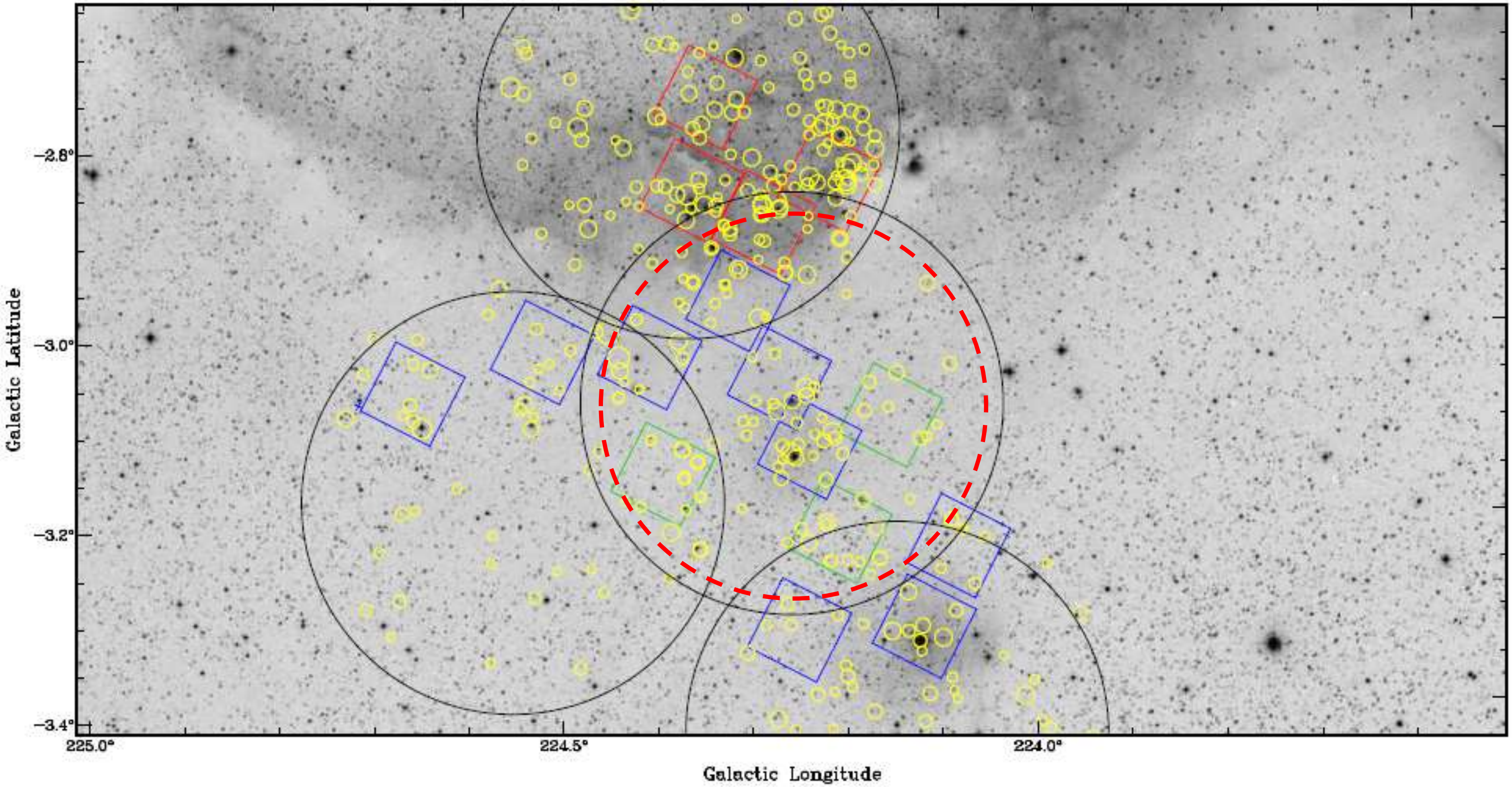

The Gemini GMOS fields (squares): Blue squares are used to indicate the new proposed observations, while green squares correspond to the fields for which the masks are ready. The red squares represent the fields where spectra have been previously acquired.

CIRCULOS EM PRETO campos XXM (X-ray). CIRCULOS EM VERMELHO: campo do VLT/FLAMES

Multi-object spectroscopy : Qual usar?

IFU ? Longslit ? Multifenda? Multifibra?

Image taken by GMOS without using the IFU

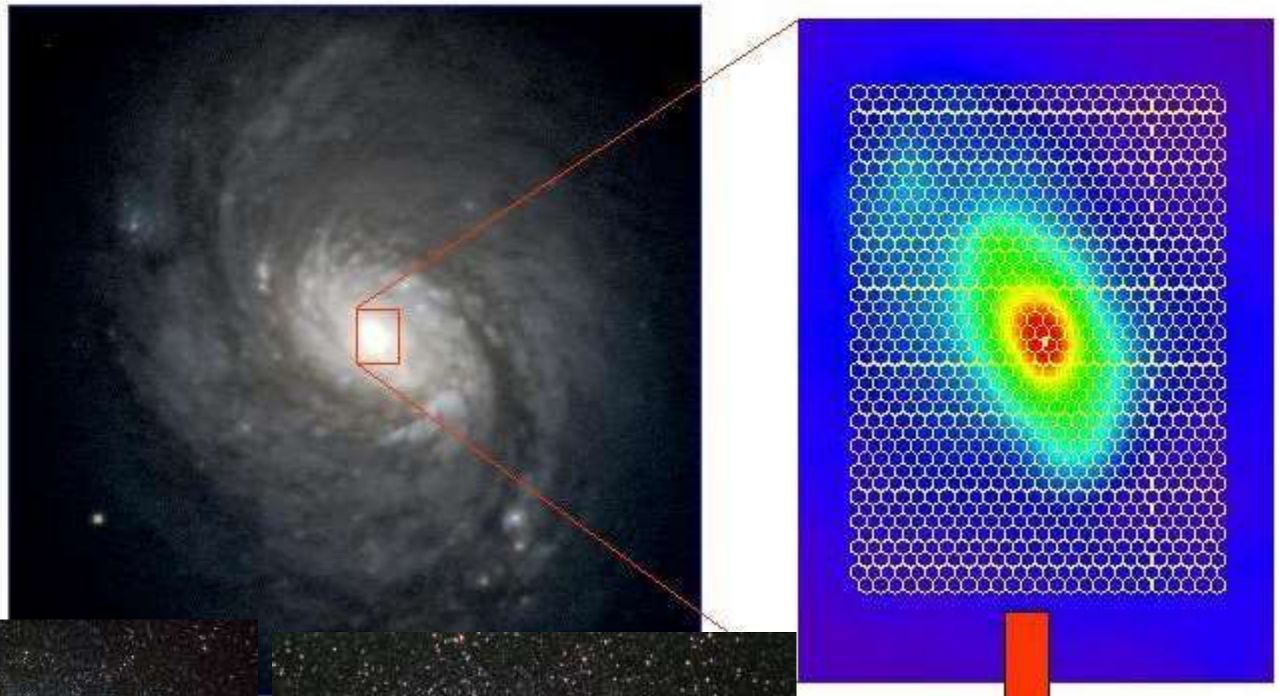

The GMOS IFU records a spectrum for each pixel

GMOS IFU Field of view 5"x7"

Aglomerados Omega Cen (left) e 47 Tuc (right) são aprox. do tamanho angular da Lua cheia